# What Explains the Rise in Intergenerational Inequality?*

Titan Alon Menaka Hampole Adam Jørring Shane McMiken

September 21, 2026

**Abstract**

Why is aggregate wealth increasingly concentrated in the hands of older households? We document that the share of aggregate wealth held by the youngest half of households fell by more than 35 percent from the 1950s to the 2010s. To understand the underlying economic mechanisms, we develop and calibrate an overlapping-generations model of the postwar United States in which human capital, factor prices, demographics, and bequests jointly shape the age–wealth distribution, and we decompose the rise in concentration using a Shapley decomposition. Rising productivity of human-capital investment accounts for essentially all of it: higher returns to skill lead young households to invest in human capital rather than save early in life, so they accumulate wealth only later. Changes in the return to physical capital account for little of it, while demographic change and transfers are, on net, concentration-reducing.

*We thank Donald Cox, Moritz Kuhn, Timothy Meyer, and seminar participants at Boston College for their valuable comments and suggestions. We thank Holly Monti and Juan Baquero Vargas for their excellent research assistance. Alon: University of California San Diego (talon@ucsd.edu), Hampole: Yale University (menaka.hampole@yale.edu), Jørring: UMass Amherst (ajorring@umass.edu), McMiken: Boston College (mcmiken@bc.edu).

# 1 Introduction

Economic pessimism is growing among young Americans, and a common concern is that older generations have accumulated most of the economy's wealth, leaving the young with little opportunity to build wealth of their own.[1] Is this concern well founded? Who owns most of the wealth in the U.S. economy, the old or the young? Has wealth become increasingly concentrated among the old, and, if so, what explains the rise? The answers to these questions have both positive and normative implications for our understanding of inequality. They also matter for the macroeconomy, as the age distribution of wealth shapes many aggregate outcomes, including economic growth and the transmission of monetary policy.[2]

To shed light on these questions, this paper measures changes in the age distribution of wealth over the post-war period in the United States and analyzes the economic forces which drive them. It documents a pronounced rise in *intergenerational inequality*: over the past seven decades, aggregate wealth has indeed become increasingly concentrated in the hands of older households. Figure 1 illustrates the central fact by plotting the net worth of younger households (under 50) and older households (50 and over) from 1950 to 2022. In 1950, older household were on average about twice as wealthy as younger households and collectively held approximately 54% of aggregate net worth; by 2022, older households were almost four times as wealthy and held 85% of aggregate net worth.

To understand the nature of these shifts, the paper combines data from the Survey of Consumer Finances with its historical extension, the SCF+ of Kuhn et al. (2020), to provide a detailed view of the changing distribution and composition of household wealth from 1949 to 2022. It develops a new statistic – the intergenerational concentration coefficient – to measure changes in wealth inequality that are robust to secular demographic change. The

[1] In a January 2024 ABC/Ipsos poll, 21 percent of adults under 30 reported that the American dream still holds true, down from 56 percent in 2010; in the April 2026 AP-NORC America 250 Poll, the corresponding share was 22 percent. In the Gallup Poll Social Series, the share of adults who consider it likely that today's youth will have a better life than their parents fell to 42 percent in 2022, the lowest since 1995.

[2] For example, see Doepke and Schneider (2006); Krueger and Ludwig (2007); Wong (2021); Mian et al. (2021); Auclert et al. (2021); Acemoglu et al. (2026).

Figure 1: Household Wealth by Age Group

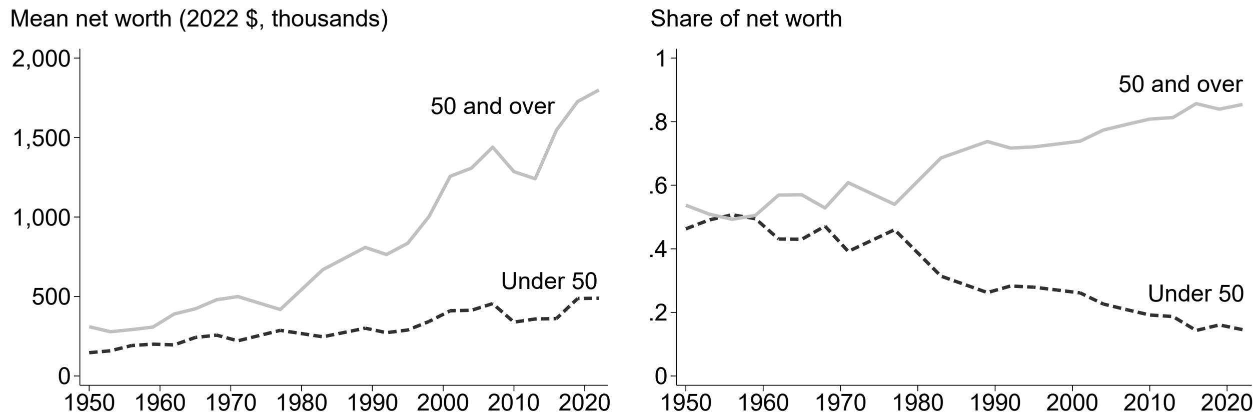


A: Mean B: Share

*Note:* The figure shows household net worth by age group from 1950 to 2022. Households are split into two groups by the age of the household head: those under 50 (black, dashed line) and those aged 50 and over (gray, solid line). Panel A plots mean net worth within each group, expressed in thousands of 2022 dollars. Panel B plots each group's share of aggregate net worth. Data source: SCF+.

statistic derives from the Lorenz curve of the age-wealth distribution, an analogue of the Gini coefficient that ranks households by age rather than wealth. In addition to be invariant to particular age cutoffs, the coefficient can also be analytically decomposed to investigate the empirical drivers of intergenerational inequality over time.

Applying the procedure to the post-war U.S. data reveals a substantial rise in the cross-age concentration of wealth. By 2022, the youngest half of households held only 22% of aggregate net worth, down 12 percentage points from the 1950s. Decomposing the aggregate change across detailed asset classes shows that the effect has been broad-based. Rather than being confined to narrow categories, such as housing, wealth concentration has increased in every asset category that can be consistently measured in the SCF+, including liabilities as well as financial and non-financial assets. While the increase in concentration is ubiquitous, the net contribution of each asset class to aggregate intergenerational inequality varies, mainly due to the changing composition of household portfolios.

Decompositions based on household characteristics reveal that education also plays a central role. The level of intergenerational wealth inequality is much higher among the college than the non-college population due, in part, to student debt, foregone earnings, and steeper lifecycle earnings profiles. As a result, the post-war rise in educational attainment lead to an increase in the aggregate cross-age concentration of wealth through a composition effect. While these human capital channels play an unambiguous role, the data show that the intergenerational concentration of wealth also increased substantially among non-college graduates, suggesting broader economic forces are also at play.

To understand the economic mechanisms driving the rise in intergenerational inequality, the paper develops a heterogeneous-agent overlapping generations model which endogenizes households' lifecycle asset accumulation. The model simultaneously considers five potential economic drivers which can explain the changing lifecycle dynamics of household net worth across subsequent cohorts in the post-war period. These include changes in real interest rates and wages; the progressivity of the tax system; the returns to human capital accumulation; intergenerational bequests; and demographic change. The set of mechanisms considered is motivated by the empirics and includes those that the review of De Nardi and Fella (2017) has shown to be important in explaining other dimensions of wealth inequality.[3]

The model builds on recent macroeconomic frameworks used to analyze the post-war rise in unconditional aggregate wealth inequality (Benhabib et al., 2019; Hubmer et al., 2021) and is adapted to focus on intergenerational wealth gaps and their welfare consequences, as in Glover et al. (2020). Accounting for the contribution of these economic channels simultaneously in a unified model is necessary since some reflect equilibrium outcomes (e.g. factor prices) while others interact non-trivially through household decision making. For example, changes in the progressivity of taxation can affect household incentives to invest in

[3]Each of the mechanisms considered has been studied elsewhere in the literature, often in isolation, and found to be an important driver of some dimensions of rising inequality (e.g., unconditional aggregates, workers versus capitalists, the top 1%, etc.). For example, for relative prices and factor demand see Karabarbounis and Neiman (2014); Acemoglu and Restrepo (2022); Moll et al. (2022); for the progressivity of taxation see Heathcote et al. (2017); Hubmer et al. (2021); Auten and Splinter (2024); for educational attainment and human capital see Huggett et al. (2011); Bartscher et al. (2020a); Alon et al. (2026); for intergenerational bequests see De Nardi (2004); De Nardi and Yang (2014); Boserup et al. (2016); Adermon et al. (2018); Nekoei and Seim (2023); for demographic change and retirement see Krueger and Ludwig (2007); De Nardi et al. (2010); Carvalho et al. (2016); Antunes and Ercolani (2020); Gagnon et al. (2021); Auclert et al. (2021).

human capital (Guvenen et al., 2014) while demographic change which increases longevity can influence the aggregate demand for savings, pushing down interest rates, and change the timing of retirement and the size of bequests (Gagnon et al., 2021; Auclert et al., 2021).

The calibration procedure estimates the parameters governing the importance of each mechanism to match the data along a perfect-foresight transition path from 1950 to 2020. The quantitative model replicates the changing lifecycle dynamics of wealth accumulation across cohorts which underlie the rise in aggregate intergenerational wealth inequality, as well as the sources of these wealth differences, including changes in lifecycle earnings, tax rates, factor prices, bequests, and the duration of working life and retirement. The contribution of each economic channel is then assessed via a Shapley decomposition which provides a unique ordering invariant and additively decomposable attribution for each the model mechanisms which exactly sum to the total change generated by the full quantitative model.[4]

The results show that all five channels considered play an important role in shaping the trajectory of intergenerational inequality. Increases in the returns to physical capital, greater investment in human capital accumulation, and decreases in the progressivity of the tax system all increased the age-wealth concentration, while bequests and demographic change moderated its rise. However, the human capital channel was unambiguously the dominant driver of the post-war rise in intergenerational wealth. In response to a secular rise in the skill premium, subsequent generations of young workers optimally prioritized investing in human capital and postponed physical savings. The resulting higher levels of student debt, greater foregone earnings, and steepening lifecycle earnings profiles which concentrate income later in life all contributed to a measured rise in intergenerational inequality.

The paper concludes by revisiting the question posed at the outset about whether the rise in intergenerational wealth inequality is a cause for concern. It does so by conducting a welfare analysis which computes the consumption-equivalent welfare variation across cohorts in the post-war period. The results show that, despite a rising concentration of wealth,

[4]See Sastre and Trannoy (2002) and Shorrocks et al. (2013) for more details on the implementation of the Shapley decomposition and its properties.

welfare increased for the majority of generations in the post-war period. Moreover, all the mechanisms analyzed with the exception of demographic change contributed, on average, to improvements in household welfare. Hence, while rising intergenerational inequality may generate negative headlines and fuel social angst, the model concludes that these shifts are largely an optimal household response to greater incentives for investment in human rather than physical capital in the latter half of the 20th century.

The paper contributes to a large empirical literature documenting the long-run evolution of income and wealth inequality in the United States (Piketty and Zucman, 2015; Saez and Zucman, 2016; Kuhn et al., 2020) and, in particular, work on the demographic and age-based dimensions of the wealth distribution (Feiveson and Sabelhaus, 2019; Gale et al., 2020; Bauluz and Meyer, 2025).[5] The paper's main result that the human capital channel is the dominant driver of intergenerational inequality connects this literature to related work showing how changes in lifecycle earnings profiles (Heathcote et al., 2010) and educational attainment (Bartscher et al., 2020a) contribute to growing wealth inequality. The findings are also conceptually important as they stand apart from leading accounts of the post-war rise in aggregate wealth inequality which attributes it predominantly to changes in the tax system, the returns to physical capital, and the revaluation of assets (Saez and Zucman, 2016, 2020; Fagereng et al., 2025; Bauluz and Meyer, 2025; Greenwald et al., 2025). The distinction is important as the welfare and policy implications of the human capital channel differ from those of the tax and financial market channels. It also motivates the development of a more encompassing measure of household wealth inequality, one that accounts for differences in human as well as physical capital (Huggett and Kaplan, 2016).

[5] Feiveson and Sabelhaus (2019) pool modern SCF waves to document life-cycle wealth trajectories, Gale et al. (2020) document the stagnation of recent cohorts, and Bauluz and Meyer (2025) extend the horizon to the 1960s, linking the transformation to the post-1980s boom in asset prices; on young households' balance sheets, see Dettling and Hsu (2014), Bartscher et al. (2020b), and McKernan et al. (2014).

# 2 The Rise in Intergenerational Wealth Inequality

This section documents the central empirical fact of the paper: over the post-war period, U.S. wealth has become increasingly concentrated in the hands of older households. To formalize this notion, we develop a measure of age–wealth concentration—the analogue of a Gini coefficient with households ranked by age rather than by wealth—and use it to characterize how the distribution of wealth across age groups has evolved since 1950. We then turn to the economic mechanisms that could account for this rise, providing descriptive evidence on the trends behind each of the four forces we study: the changing returns to physical capital and to labor, demographic change, bequests and inter vivos transfers, and the rising returns to human-capital investment.

Our analysis draws primarily on the Survey of Consumer Finances (SCF) and its historical extension, the SCF+. The modern SCF is a triennial cross-section of U.S. household balance sheets spanning 1989 to 2022; the SCF+ of Kuhn et al. (2020) extends consistent, reweighted balance-sheet data back to 1949, giving us a harmonized view of household wealth across the age distribution over more than seven decades. We defer the details of dataset construction, variable imputations, and the supplemental demographic and macro-financial data to Appendix A.I, where Table D.1 reports summary statistics.[6]

## 2.1 The Age-Wealth Concentration Curve

We represent the age-wealth distribution by the *age-wealth concentration curve*: the curve which plots the cumulative share of wealth against the cumulative share of households ranked from youngest to oldest. In general, a concentration curve is similar to a Lorenz curve except it allows a researcher to analyze how a variable like household age relates to the wealth distribution. In our setting, let X denote net wealth and Y denote the household age. The

[6] Because defined-benefit (DB) pension wealth is largely absent from the raw surveys yet is sizable in the portfolios of older households, we augment net worth with imputed DB wealth—following Sabelhaus and Volz (2022) for the modern waves and Bauluz and Meyer (2025) for the historical waves—and we express all values in constant 2022 dollars.

*age-wealth concentration curve* is defined by

$$L_{XY}(p) = \frac{\int_{-\infty}^{p} \int_{-\infty}^{\infty} f_{XY}(x, y) dx dy}{\mu_X} \tag{1}$$

where $p$ is the percentile of the distribution of households by the age of their head and $f_{XY}(x, y)$ is the density of the joint distribution of age and wealth. For a given percentile $p$, the concentration $L_{XY}(p)$ is read as the cumulative share of total net wealth owned by households ranked $p$-percentile in the age distribution and below.

The *age-wealth concentration coefficient* of the age-wealth concentration curve is a statistic which summarizes the inequality in wealth over the distribution of age. The concentration coefficient has the same geometric interpretation as the familiar Gini coefficient, which is equal to the area between the concentration curve and the 45-degree line as a proportion of the total area underneath the 45-xdegree line. The covariance based formulation for the concentration coefficient is given by

$$C_{XY} = -2\text{Cov}\left(\frac{X}{\mu(X)}, (1 - F_Y(Y)\right) \tag{2}$$

where $F_Y(y) = \int_{-\infty}^{y} \int_{-\infty}^{\infty} f_{XY}(x, y') dx dy'$ is the cumulative density function of household head's age. Intuitively, $C_{XY}$ is proportion to the distance of the distribution of net wealth over age from the uniform distribution. A more positive value indicates wealth is more concentrated among older households, whilst a more negative value can indicate either a less concentrated distribution or even a wealth distribution where wealth is concentrated among the young.

Figure 2 documents our main result, revealing that wealth has become more concentrated among older households in the past 70 years. Specifically, we plot equation (1) combining the SCF+ and SCF survey waves for the 1950s and the 2010s. Comparing the two curves, we see a large increase in age-wealth inequality. That is, for every age percentile between the 5 to 85 percentile, the curve for the 1950s lies above the curve for the 2010s. For example, in

Figure 2: The Rise of Intergenerational Wealth Inequality

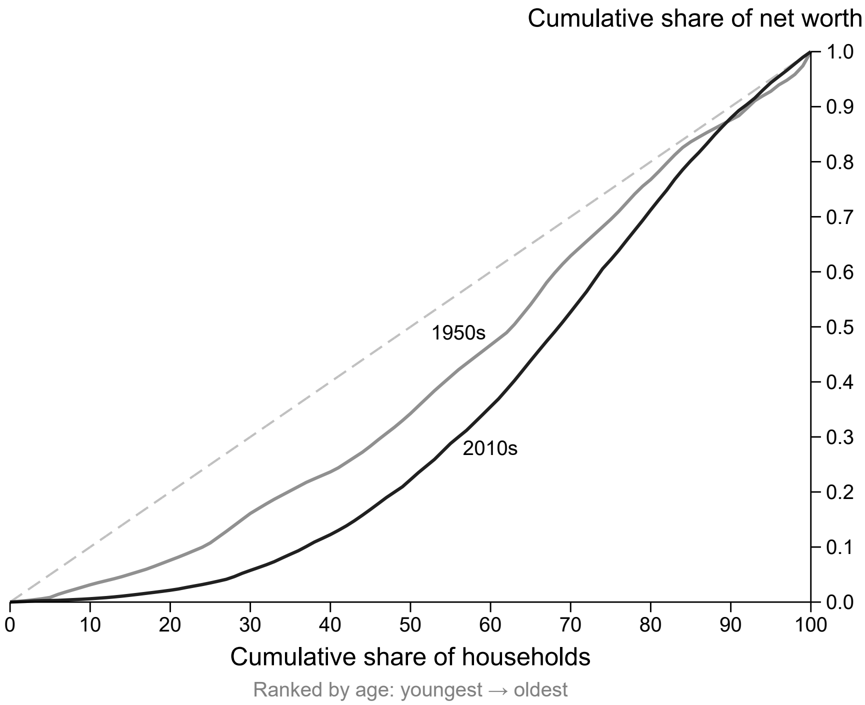


*Note:* This figure plots age–wealth concentration curves for the 1950s and 2010s: the cumulative share of household net worth held (vertical axis) against the cumulative share of households ranked from youngest to oldest (horizontal axis). The dashed line is the 45° line; curves farther below it indicate wealth more concentrated among older households. The 1950s curve pools the 1950, 1953, 1956, and 1959 survey waves; the 2010s curve pools 2010, 2013, 2016, and 2019. Data source: SCF+.

the 1950s the 50 percent youngest households own 34% of wealth, whereas in the 2010s the 50 percent youngest households only own 22% of the wealth. The advantage of comparing concentration curves, instead of relying on a simple age cut-offs, is that we are able to comment on the change in age-wealth distribution without having to make specific reference to particular age groups.

Figure C.1 plots the age–wealth concentration coefficient by decade from the 1950s to the 2010s, together with a 90% confidence band obtained as the 5th and 95th percentiles of the coefficient recomputed across 999 bootstrap replicate weights. The figure reveals a surprising pattern for the latter part of the sample: We find that the age-wealth concentration curve has remained constant between the 1980s and 2010s. This is in stark contrast with the literature studying absolute wealth inequality which highlights the increase in inequality following the

1980s.

Taken together, these two stylized facts establish the motivating empirical result of the paper. The distribution of net worth across age groups has grown markedly more unequal: the youngest half of households held 34% of net worth in the 1950s but only 22% by the 2010s, and the age–wealth concentration coefficient rose steadily over the same period. This increase, however, occurred almost entirely before 1980 and has been essentially flat since. That timing is the reverse of headline wealth inequality, which was stable through the 1970s and rose sharply thereafter, so the rise in older households' share of wealth was largely complete before the post-1980 asset boom that dominates the conventional account. We next turn to the economic forces that could have driven this earlier rise, presenting descriptive evidence on the trends behind each of the candidate mechanisms: the return to physical capital, the return to labor, demographic change, bequests and inter vivos transfers, and the returns to human-capital investment, which we later embed in the model.

## 2.2 Potential Economic Mechanisms

The rise in age–wealth concentration could in principle reflect any of several distinct economic forces. In this subsection we take each candidate mechanism in turn and ask whether the trend underlying it moved in the direction, and over the period, that the concentration coefficient did. The evidence here is descriptive: because these forces operate at once and interact in general equilibrium, the raw trends can indicate which mechanisms are plausible but cannot, on their own, apportion the rise among them. That accounting is the task of the structural model developed in the next section, which disciplines each force with these same data and quantifies its contribution through a Shapley decomposition.

**Returns to Human-Capital Investment.** The first mechanism is the rising return to human-capital investment. Over the post-war period the return to skill rose and educational attainment expanded as successive cohorts completed more schooling (Katz and Murphy, 1992; Goldin and Katz, 2008). In the human-capital model, a higher return to skill, $z$, induces young households to invest more in human capital—forgoing early-career earnings and saving while in school or training—which steepens life-cycle earnings profiles and shifts the earnings households realize, and the saving it finances, toward middle age (Ben-Porath, 1967).[7] Panel A of Figure 3 shows the steepening directly in our data: plotting mean income by age separately for the Silent Generation, Baby Boomers, Generation X, and Millennials, each successive cohort earns less early in life and more later, so that the age profile of income—and of the saving it finances—grows progressively steeper across cohorts. A rise in $z$ thus raises the concentration of wealth among older households, by suppressing young households' early physical saving while raising the earnings, and hence the assets, accumulated later in life.

**Demographic Change.** A second mechanism is demographic. Life expectancy at older ages rose steadily over the post-war period—at age 65 from roughly 14 years in 1950 to roughly 20 by the 2010s—and the population aged as fertility fell and large cohorts moved through the age distribution (Bloom et al., 2003; Poterba, 2001). Panel B of Figure 3 plots the adult age distribution in the 1950s against the 2010s: the share of adults aged 65 and over rose from 12.6% to 18.4%, while the share aged 18–34 fell from 36.3% to 30.8%. A longer expected retirement raises the assets households must accumulate before they stop working and slows the rate at which they draw those assets down, raising measured wealth at older ages (Modigliani, 1986).[8] Both channels raise the concentration of wealth among the old, and Antunes and Ercolani (2020) attribute one-third to one-half of the rise in across-age

[7]This logic rests on the foundational human-capital tradition (Becker, 1964; Mincer, 1974; Card, 1999) and on a macro-labor literature relating the rising skill price to the widening wage structure and steepening life-cycle profiles (Guvenen and Kuruscu, 2012). The expansion of attainment and the steepening of profiles are concentrated around mid-century, ahead of the post-1980 forces discussed below (Restuccia and Vandenbroucke, 2013; Hendricks and Schoellman, 2014).

[8]The slow drawdown of wealth at older ages, relative to the canonical life-cycle benchmark, is itself attributed to longevity risk and late-life medical expenses (De Nardi et al., 2010). Population aging raises the share of households in the high-wealth older age groups (Auerbach and Kotlikoff, 1987; Auclert et al., 2021), and the same demographic forces have been linked to the secular decline in real interest rates (Eggertsson et al., 2019; Gagnon et al., 2021; Carvalho et al., 2016; Krueger and Ludwig, 2007).

Figure 3: Human Capital and Demographic Change

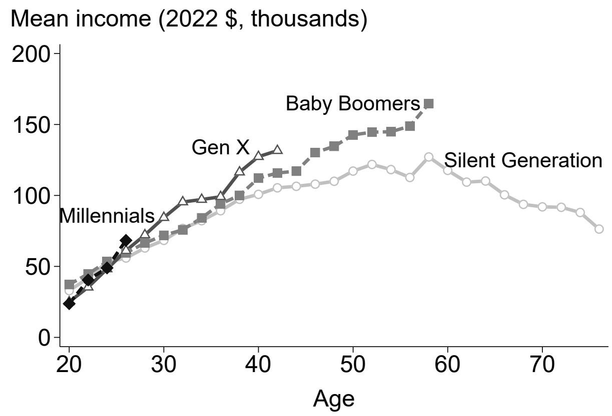


A: Income by cohort

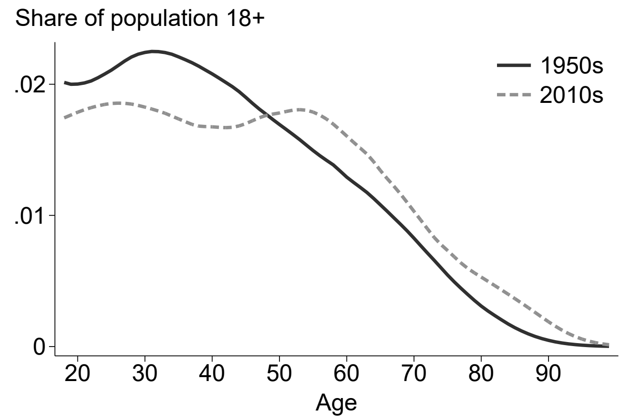


B: Adult age distribution

*Note:* Panel A plots mean household income by the age of the household head, separately for four birth cohorts defined by the head's year of birth: the Silent Generation (1928–1945), Baby Boomers (1946–1964), Generation X (1965–1980), and Millennials (1981–1996). Income is expressed in thousands of 2022 dollars, and each cohort is shown over the age range for which it is observed in the SCF+ through 2022. Panel B plots the age distribution of the U.S. adult population, ages 18 and over, in the 1950s (solid) and the 2010s (dashed); each point is a single year of age's share of the 18-and-over population, averaged with equal weight across the ten years of the decade. Data sources: SCF+ (Panel A); United Nations World Population Prospects 2024 (Panel B).

wealth inequality to them. The magnitude of the net demographic effect is less clear, for two reasons. The demographic shift is gradual, spread across the full horizon rather than concentrated in the decades over which the coefficient rose; and because our measure ranks households by their position in the age distribution rather than by fixed age cutoffs, it adjusts for secular demographic change, so a uniform aging of the population moves it far less than it moves age-threshold wealth shares.

**Relative Returns to Capital and Labor.** The third mechanism operates through factor prices: the return to physical capital relative to labor. This is the channel emphasized in the literature on aggregate wealth inequality, which attributes much of the post-war rise to the returns to capital and to the revaluation of existing assets (Piketty and Zucman, 2014). On the capital side, the real return to wealth has been high but volatile, and its most pronounced movement is a post-1980 revaluation: falling discount rates lifted the market value of existing equities, housing, and long-duration bonds, which, because such assets

Figure 4: Returns to Physical Capital

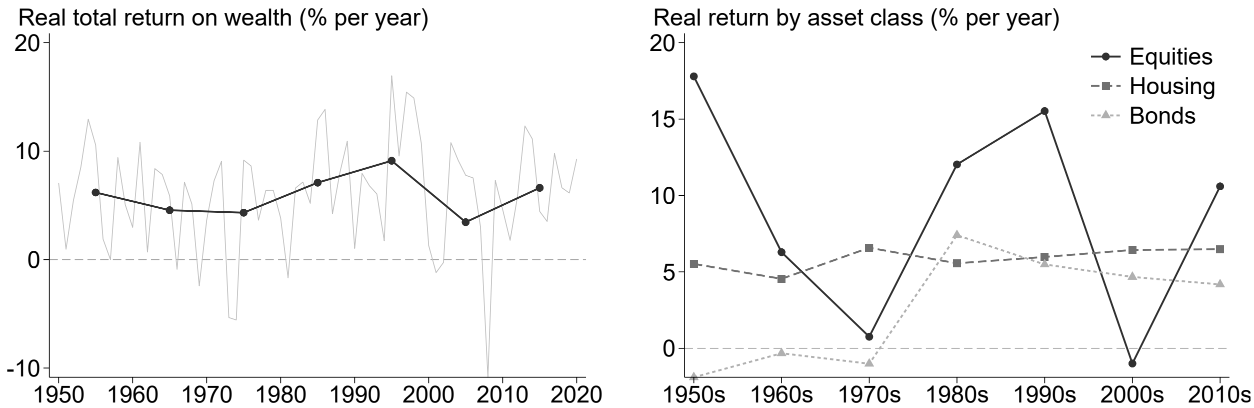


A: Total return

B: By asset class

*Note:* This figure shows the real return on U.S. wealth from 1950 to 2022, expressed in percent per year and deflated by the CPI. Panel A plots the real total return on wealth: the faint line is the annual series and the heavy line with markers is the decade mean (1950s through 2010s). Panel B decomposes the real return by asset class—equities, housing, and bonds—reported as decade means over the same period. Data source: Jordà–Schularick–Taylor Macrohistory Database.

are held disproportionately by older households, raises old-age wealth relative to young-age wealth (Fagereng et al., 2025; Greenwald et al., 2025).[9] Figure 4 plots the realized return over our sample: Panel A shows the real total return on wealth, which fluctuates sharply year to year and, averaged by decade, displays no secular trend over the 1950s–80s; Panel B decomposes the return into equities, housing, and bonds, whose decade averages likewise move substantially without a common low-frequency rise. On the labor side, the U.S. labor share of income was broadly stable through the early post-war decades and then declined after about 1980 (Karabarbounis and Neiman, 2014; Elsby et al., 2013).[10] Figure 5 documents the two facts most relevant here: Panel A shows that real hourly compensation increasingly lagged labor productivity, and Panel B shows the decline in the labor share. To the extent that older households hold capital while younger households rely on labor income, a rising return to capital and a falling return to labor both raise the wealth of the old relative to the

[9] A related literature attributes much of the recent growth in top wealth to asset-price revaluation rather than to active saving (Gomez, 2025; **?**; Hubmer et al., 2021; Saez and Zucman, 2016).

[10] The decline has been attributed to the reallocation of activity toward low-labor-share firms and rising markups (Autor et al., 2020; De Loecker et al., 2020) and to labor-replacing automation (Acemoglu and Restrepo, 2022; Stansbury and Summers, 2020).

Figure 5: Returns to Labor

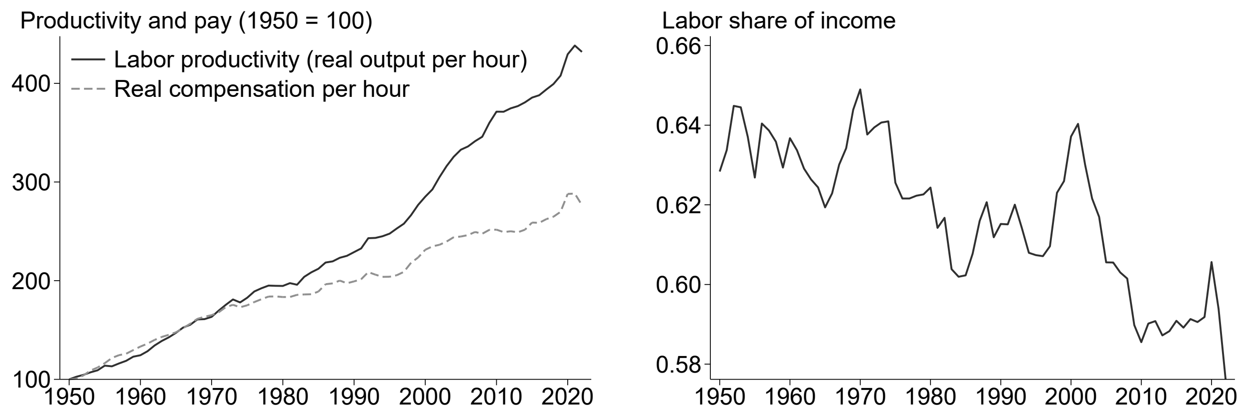


A: Compensation and productivity

B: Labor share

*Note:* This figure shows the price of labor in the U.S. from 1950 to 2022. Panel A plots real hourly compensation and labor productivity (real output per hour) in the U.S. nonfarm business sector, each indexed to 100 in 1950. Panel B plots the U.S. labor share (share of labor compensation in GDP). Data sources: U.S. Bureau of Labor Statistics (Panel A); Penn World Table (Panel B).

young.

**Bequests and Intergenerational Transfers.** The final mechanism is intergenerational transfers—bequests and inter vivos gifts. Transfers account for a sizable, if contested, share of aggregate wealth (Kotlikoff and Summers, 1981; Modigliani, 1988), and they flow predominantly from older to younger households, arriving before recipients would have accumulated comparable wealth through life-cycle saving alone (Nekoei and Seim, 2023).[11] By front-loading resources onto the young—raising the wealth of households that life-cycle saving alone would leave asset-poor—transfers reduce the gap in wealth between old and young (Boserup et al., 2016; De Nardi, 2004).[12] An increase in the incidence or size of transfers therefore lowers, rather than raises, the concentration of wealth among older households; for this mechanism to have contributed to the observed rise, transfers to the young would have

[11] See also Gale and Scholz (1994) on the share of aggregate wealth attributable to transfers and Adermon et al. (2018) on the share of the parent–child wealth correlation that runs through inheritances and gifts.

[12] Boserup et al. (2016) find that bequests raise absolute dispersion but lower relative wealth inequality; Nekoei and Seim (2023) find that inheritances reduce relative inequality on receipt, though the effect attenuates as wealthier heirs retain more. See also Becker and Tomes (1979) and the survey of De Nardi and Yang (2014).

had to contract over the period.

## 3 A Model of Intergenerational Inequality

This section presents the quantitative model used to analyze the rise in intergenerational inequality. To do so, the model endogenizes the lifecycle accumulation of assets underlying the stylized facts documented in section 2. Consistent with that evidence, it contains four potential mechanisms to explain changes in the aggregate distribution of assets across cohorts and age groups. These include increases in the returns to human capital which incentivize young workers to accumulate human rather than physical capital; changes in factor prices including the returns to capital and wages; demographic shifts which change the age composition and the relative length of working life and retirement; and shifts in the initial assets of young households due to bequests and intergenerational transfers.

**Households.** The economy is populated by overlapping generations of finitely-lived, heterogeneous agents who make consumption, savings, and human capital investment decisions. Each period corresponds to a decade with $t$ indexing time and $j$ indexing age. All households are forward-looking with rational expectations and can be identified by their time $t$ state vector $(h, a, j)$ denoting their prevailing human capital, asset holdings, and age. The decision problem for working individuals is given by,

$$V_{j,t}(h_t, a_t) = \max_{c_t, s_t, a_{t+1}} \; u(c_t) \; + \; \beta \mathbb{E}_{j,t}\big[V_{j+1,t+1}(h_{t+1}, a_{t+1})\big] \tag{3}$$

subject to the budget constraint and human capital technology given by,

$$c_t + a_{t+1} = R_t a_t + W_t(1 - s_t)h_t \tag{4}$$

$$h_{t+1} = z_t(s_t h_t)^\alpha + (1 - \delta)h_t \tag{5}$$

$$a_{t+1} \geq \bar{a} \quad , \quad 0 \leq s_t \leq 1 \tag{6}$$

where $c_t$ denotes consumption, $a_t$ assets, and $h_t$ human capital. Parameter $\bar{a}$ represents the exogenous household borrowing limit. Households can accumulate human capital through costly time investments $s_t$ according to the Ben-Porath (1967) technology in (5), subject to depreciation rate $0 < \delta < 1$. Parameter $z_t$ is the productivity of the learning technology which determines the pecuniary returns to human capital investment. The gross return on physical capital is denoted by $R_t$ and the effective wage rate is given by $W_t$. Finally, households have rational expectations and correctly forecast future aggregate and age-specific shocks so that the expectation operator is indexed by age $j$ and time $t$. The initial distribution of assets, $a_0$, of newly entering cohorts at time $t$ is denoted by $\mathcal{F}_t(a_0)$.

**Retirement.** Individuals retire at the end of working life and live off of their accumulated savings. They may also stochastically enter retirement earlier in their working life (see next section). Retired households continue to make consumption and savings decisions, but no longer earn labor income or invest in human capital. Additionally, retired households also have a bequest motive in deciding how much assets to leave for their progeny. Formally, the decision problem of a household which retired with assets $a_t$ is given by,

$$V^r(a_t) = \max_{a_{t+1}} \; u(c) \; + \; \beta \left[(1 - \pi^d)V^r(a_{t+1}) + \pi^d V^b(a_{t+1})\right] \tag{7}$$

subject to the budget constraints

$$c_t + a_{t+1} \;=\; R_t a_t \tag{8}$$

$$a_{t+1} \;\geq\; \bar{a} \tag{9}$$

While retired, households face a stationary Poisson probability of dying, $\pi_d$. With probability $1-\pi_d$ they survive another period and continue to live off their savings. With probability $\pi_d$, they pass away and bequeath their remaining assets. Following De Nardi and Yang (2014) and Blundell et al. (2016), the bequest motive is modeled in reduced form. Specifically, the value of leaving bequests $a_{t+1}$, $V^b(a_{t+1})$, is given by

$$V^b(a_{t+1}) \;=\; \phi_t u(a_{t+1}) \tag{10}$$

In other words, the value of a bequest is proportional to the consumption value of bequeathed assets, where $\phi$ parameterizes the strength of the retired household's bequest motive.

**Demographics.** Household economic decision making begins at age 20 when the cohort specific distribution of initial assets $a$ and $h_0$ is realized. Households age deterministically. Working individuals retire stochastically with Poisson rate $\pi^r_{j,t}$ which can vary by age and over time.[13] Retired households face a Poisson probability of death, $\pi^d_t$, which can vary over time to capture changes in lifespans, and hence the length of retirement, over the period we study. Capturing the retirement and mortality margins are important as retired households do not earn labor income and so longer periods of retirement imply a greater incentive to accumulate assets during working life to finance consumption during retirement. These incentives are therefore first order in determining asset holdings across the age distribution and thereby shape the intergenerational distribution of asset holdings the model focuses on.

The model also captures changes in the economy's demographic distribution over time by accounting for the relative size of entering cohorts. The size of each new entering cohort at time $t$ is given by its population share $\omega_{1,t}$. The relative size of any cohort is also allowed to vary over time due to, among other things, premature death or migration. The relative size of any cohort age $j$ at time $t$ is given by its population share $\omega_{j,t}$. The demographic structure of the model therefore allows it to capture changes in the relative size of cohorts via the $\omega_{j,t}$, changes in participation rates over the lifecycle via $\pi^r_{j,t}$, and changes in the relative length of working life versus retirement via $\pi_t$.

[13] All working individuals retire deterministically by age 80 if they have not already done so.

**Production Technology and Firms.** Aggregate output $Y_t$ is produced by a competitive sector of profit-maximizing firms. The production technologies exhibit constant returns to scale and a constant elasticity of substitution (CES) between capital and labor, the two primary factors of production. Formally, the technology is given by

$$Y_t = \left[ (A_{k,t} K_t)^{\frac{\sigma-1}{\sigma}} + (A_{l,t} L_t)^{\frac{\sigma-1}{\sigma}} \right]^{\frac{\sigma}{\sigma-1}} \tag{11}$$

where $A_{k,t}$ and $A_{l,t}$ represent capital-augmenting and labor-augmenting technology, respectively, $K_t$ is aggregate capital, $L_t$ is aggregate effective labor, and $\sigma$ captures the elasticity of substitution between the two factors of production.[14]

By modeling the production sector, the model endogenizes the determination of factor prices for capital and labor in general equilibrium. As a result, when the savings and human capital investment behavior of one cohort changes, it will feed back into the decisions of other cohorts at different points in their lifecycle. For instance, if older cohorts are accumulating more physical assets, it will depress the returns on capital and raise the return to human capital investments for subsequent young cohorts. This allows the model to capture additional linkages between the savings behavior across cohorts which determine the level of intergenerational inequality through the equilibrium determination of factor prices. The model additionally allows for exogenous changes in factor-augmenting productivities $A_{k,t}$ and $A_{l,t}$ to fully capture the path of wages $W_t$ and returns on capital $R_t$ observed in the data. The counterfactuals below which decompose the rise in intergenerational inequality therefore fully account for the role of factor prices and how they might change due to exogenous and endogenous factors during the period we analyze.

[14]The effective labor of any worker $i$ is given by $(1 - s_i)h_i$, which depends on both the time they allocate to work and their prevailing human capital.

# 4 Calibration and Model Fit

The calibration sets the model parameters to replicate the documented rise in intergenerational inequality and discipline the four economic mechanisms determining changes in the cross-age distribution in asset holdings over time. It characterizes these changes as a perfect-foresight equilibrium transition path from 1950 to 2020. Four sets of parameters are allowed to change over time to drive changes in cross-cohort lifecycle savings behavior. These include, changes in the return to human capital investments $\{z_t\}_{t=0}^{\infty}$; changes in factor productivities $\{A_{k,t}, A_{l,t}\}_{t=0}^{\infty}$; changes in the timing of retirement and demographics $\{\omega_{j,t}, \pi_{j,t}^r, \pi_t^d\}_{t=0}^{\infty}$; and changes in bequest behavior and initial asset distribution $\{\mathcal{F}_t, \beta_t, \phi_t\}_{t=0}^{\infty}$. The following subsections report the model fit and explain how each of the model parameters is determined.

**External Calibration.** Three parameters governing household preferences, the elasticity of substitution between capital and labor in the production technology, and the depreciation of human capital are set externally from evidence in the literature. The coefficient of relative risk aversion $\gamma$ is set to 1.125, consistent with the evidence presented in Chetty (2006). The depreciation rate of human capital $\delta$ is set to 0.355, matching the annualized depreciation rate of 4.3% estimated by Dinerstein et al. (2022). Finally, the elasticity of substitution between capital and labor in the aggregate production technology $\sigma$ is set to 0.6, the midpoint of the range of values documented in the literature meta-analysis of Knoblach and Stöckl (2020). Table D.6 in the appendix summarizes the parameter estimates and their sources.

The parameters $\{\omega_{j,t}, \pi_{j,t}^r, \pi_t^d\}_{t=0}^{\infty}$ are also set exogenously to replicate the changing demographic, mortality, and retirement dynamics observed over the sample period. The retirement rates $\pi_{j,t}^r$ are computed from the ACS to capture changing labor force participation rates across the age distribution over time. The time varying mortality rate $\pi_t^d$ of retired households is set using data from the Social Security Administration's (SSA) life tables and Munnell (2025)'s retirement age series to match the average life expectancy of households following retirement. Finally, the aggregate demographic structure of the economy is set to match the cross-sectional population weights, $\omega_{j,t}$, derived directly from the empirical demographics reported in the SCF. Table D.7 in the appendix reports the resulting demographic parameter values and how they evolve over time.

**Internal Estimation.** The remaining parameters $\{\alpha, z_t, \mathcal{F}_t, \beta_t, \phi_t, A_{k,t}, A_{l,t}\}_{t=0}^{\infty}$ are fit jointly within the model to replicate the time path of lifecycle savings, earnings, demographics, and factor prices along the transition path from 1950 to 2020. While all the parameters will jointly determine the set of targets used in the calibration, the exposition which follows builds intuition by discussing the parameters in sets alongside the data targets most closely associated with their identification. Table D.7 in the appendix reports the estimated values for all the internally set parameters. Appendix B provides additional details on the calibration methodology and data targets.

The shape of household lifecycle earnings profiles are primarily determined by parameters $\alpha$ and $z_t$ of the human capital technology. They are therefore set to replicate the concurrent steepening of household earnings profiles accompanying the rise in intergenerational inequality, as documented in section 2. Figure 6 displays the data moments and model fit; Table D.8 reports the specific data targets and model moments underlying the figure. Parameter $\alpha$ controls the elasticity of human capital with respect to time investments in skill acquisition, $s_t$, and does not change over time.[15] Similarly, productivity parameter $z_t$ determines the amount of income-augmenting human capital individuals accumulate for a given time investment. Since human capital investment is costly in terms of foregone earnings, increases in $z_t$ lead to a steepening of household earnings profiles by stimulating investment that decreases current income but leads to faster earnings growth. Despite being common across age groups, changes in $z_t$ will disproportionately effect the earnings trajectory of young households who have the longest working life horizon and therefore invest the most time $s_t$ in human capital accumulation.

[15]Human capital investments, $s_t$, are not directly observable in the data and hence the lifecycle earnings data only provide a single degree of freedom to be fit over time. As in much of the literature, the calibration therefore holds the elasticity of investment $\alpha$ constant and uses changes in productivity $z_t$ to match the data.

Figure 6: Cohort Earnings Life-Cycles: 1950–2010

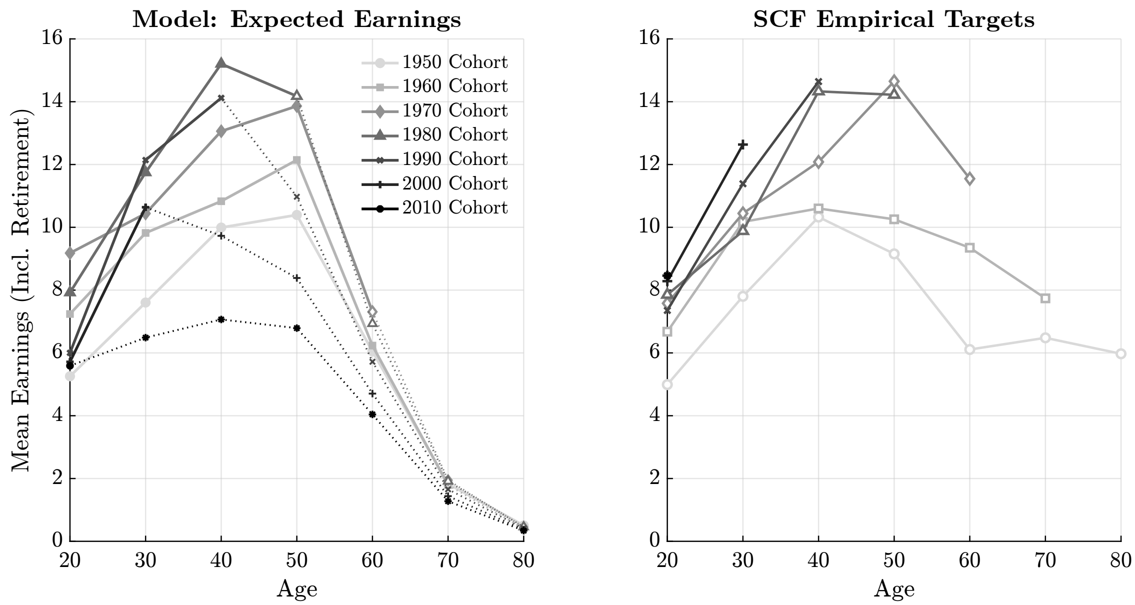


*Note:* This figure illustrates the life-cycle earnings trajectories for seven overlapping generations: cohorts entering the workforce (age 20) between 1950 and 2010. The left panel displays the structural model's simulated paths, while the right panel plots the corresponding empirical targets derived from the Survey of Consumer Finances (SCF), scaled to decade flows. To distinguish cohorts across the transition path, the plotted series utilize a grayscale gradient, transitioning from light gray for the oldest cohort (1950) to solid black for the youngest (2010). Model-implied paths are denoted by solid lines with square markers, transitioning to dotted segments for projections extending beyond the 2010 active calibration window. Empirical data are plotted with solid lines and circular markers. Table D.8 in the appendix reports the exact targets and model moments underlying this figure.

The initial distribution of assets $\mathcal{F}_t$, the discount factor $\beta_t$, and the bequest motive $\phi_t$ primary determine the lifecycle accumulation of assets. Figure 7 displays the data moments and model fit; Table D.9 reports the specific data targets and model moments underlying the figure. All three parameters are cohort-specific and fixed over the lifecycle for those entering at time $t$ and are set to match evidence from the Survey of Consumer Finances (SCF). The initial distribution of assets $\mathcal{F}_t$ for newly entering cohorts at time $t$ is set non-parametrically to replicate the initial asset holdings of workers ages 20 to 30 observed in the data. Given initial assets, the cohort-specific discount factor $\beta_t$ will determine household savings behavior via the Euler Equation. The discount factor for those entering the model at time $t$ is set

Figure 7: Physical Assets Life-Cycles

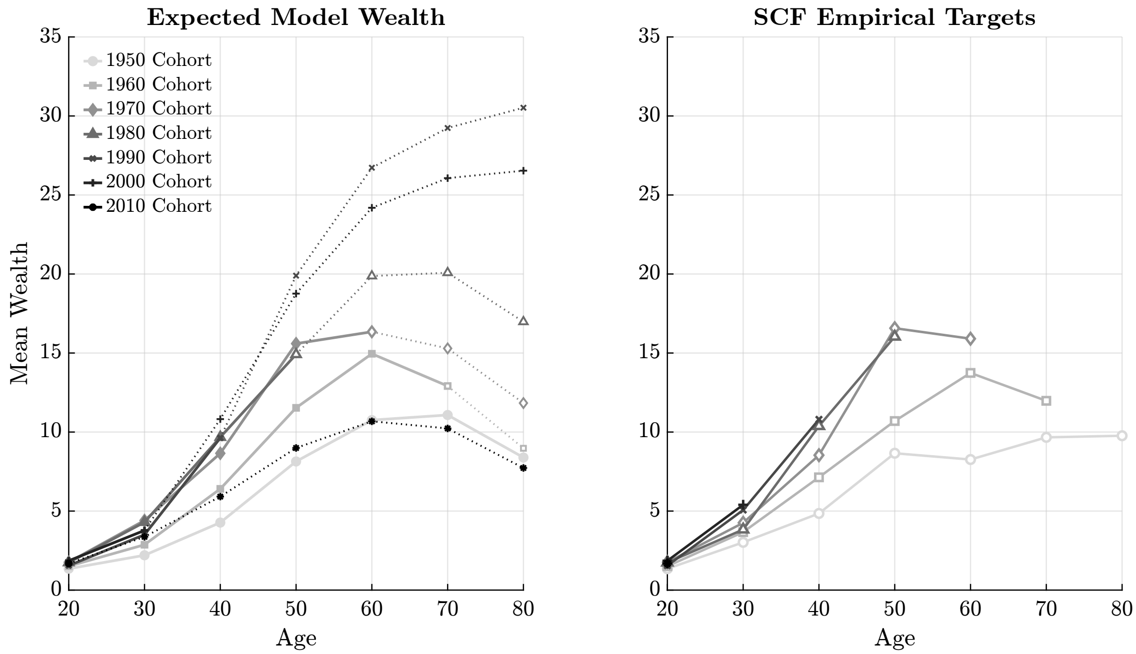


*Note:* This figure illustrates the physical asset accumulation trajectories over the life-cycle for cohorts entering the workforce (age 20) in 1950 and 2000. Dashed lines with circular markers represent empirical targets derived from the Survey of Consumer Finances (SCF). Solid lines with square markers denote the realized life-cycle paths simulated by the structural model, while dotted segments indicate model projections for cohort-years that extend beyond the active 2020 calibration window into the terminal steady state. Table D.9 in the appendix reports the exact targets and model moments underlying this figure.

to replicate the speed of asset accumulation over the lifecycle for each cohort by targetting the asset holdings of retired households.[16] The bequest motive parameter $\phi_t$ determines the degree to which retired household consume their accumulated assets versus retaining them for bequests. Parameter $\phi_t$ are set to match the average size of terminal life assets left by each cohort. Finally, note that while intergenerational household linkages are not explicitly specified, the model is nevertheless implicitly consistent with the realized bequest patterns in the data by replicating the evolution of initial assets, lifecycle asset accumulation, and size of bequests across cohorts over time.

The final set of internally calibrated parameters are the factor productivities for capital

[16] As such, shifts in $\beta$ across cohorts should be interpreted broadly as encompassing all cross-cohort changes in savings motives not explicitly modeled, such as changes in family structure, child-rearing, precautionary savings, and evolving social norms regarding wealth accumulation.

$A_{k,t}$ and labor $A_{l,t}$. These parameters are chosen to exactly replicate the path of wages $W_t$ and the returns on capital $R_t$ in the data. The aggregate returns on physical capital are computed for each decade using the Macro-History database assembled by Jordà et al. (2017). Given the production technology, household human capital and savings behavior will be jointly determined with factor prices in equilibrium. That is, household human capital and savings behavior will shape the aggregate supply of capital and labor determining prices; while the trajectory of prices in turn feed back into household decisions to save and accumulate human capital. Without additional restrictions, the prevailing equilibrium factor prices may be counterfactual even when the household lifecycle of earnings and assets matches the data. To ensure this is not the case, the calibration sets the exogenous path for capital and labor productivities along the transition path to exactly replicate the observed path of wages and interest rates over time, given households' endogenous savings and investment behavior.

# 5 Quantitative Results

Using the quantitative model, this section presents a structural decomposition of the rise in intergenerational inequality from the 1950s to the 2010s. The results report the contribution of each of the model's four constituent drivers–the returns to human capital, demographic change, the relative returns to capital and labor, and bequests and transfers–to the observed rise in wealth inequality during this period. Following section 2, the main object of analysis to be decomposed is the age-wealth concentration coefficient defined in equation (2) which summarizes the state of intergenerational inequality. Appendix figure C.12 demonstrates that the quantitative model accurately captures the rise in the coefficient over time, despite not being directly targeted in the calibration.

## 5.1 Decomposing Intergenerational Inequality

To achieve an exact, order-independent decomposition, we adapt the decomposition Shapley decomposition framework of Shorrocks et al. (2013) and Sastre and Trannoy (2002).[17] Formally, let $C_{XY}(S)$ denote the age-wealth concentration coefficient generated by a counterfactual economy driven by a subset of mechanisms $S \subseteq \mathcal{M}$. The resulting evolution of the wealth concentration coefficient $C_{XY}$ between the baseline period $t_0$ (represented by the empty set $\emptyset$ where all mechanisms are frozen) and the final period $t_1$ (represented by all mechanisms $\mathcal{M}$) is given by $\Delta C_{XY} = C_{XY}(\mathcal{M}) - C_{XY}(\emptyset)$. Considering all possible combinations of economic mechanisms, the Shapley value $\phi_m$ maps the unique attribution of the global change $\Delta C_{XY}$ to mechanism $m \in \mathcal{M}$. It is computed as the weighted average of the marginal contributions of mechanism $m$ across all possible sub-sets of mechanisms which include $m$. Formally,

$$\phi_m = \sum_{S \subseteq \mathcal{M} \setminus \{m\}} \frac{|S|!\,(M - |S| - 1)!}{M!} \Big( C_{XY}(S \cup \{m\}) - C_{XY}(S) \Big) \tag{12}$$

where $M = |\mathcal{M}| = 4$ represents the complete set of structural mechanisms considered in the model. The weight $\frac{|S|!(M-|S|-1)!}{M!}$ corresponds to the probability that mechanism $m$ is introduced into the simulation after a randomly ordered sequence of all other mechanisms.

The Shapley decomposition has two advantages relative to alternative approaches. First, it provides an unique additively decomposable attribution for each the model mechanisms which exactly sum to the total change generated by the full quantitative model. Second, it is invariant to the ordering with which the various mechanisms are assessed. In contrast, the more common leave-one-out or add-one-in decompositions would provide different attributions to each of the model's mechanisms as they interact non-linearly within the model. The methodology here therefore provides an exact decomposition of rising intergenerational

[17] Originally developed in cooperative game theory to assign a unique and fair payout to players in a coalition, the methodology has been adapted for distributional analysis and inequality accounting by Shorrocks et al. (2013) and Sastre and Trannoy (2002). See also Audoly et al. (2025). It is also used variously in the spatial/network literature Allen and Arkolakis (2014); Henderson et al. (2018); Shepard (2022)

Figure 8: Drivers of Age-Wealth Concentration (1950s–2010s)

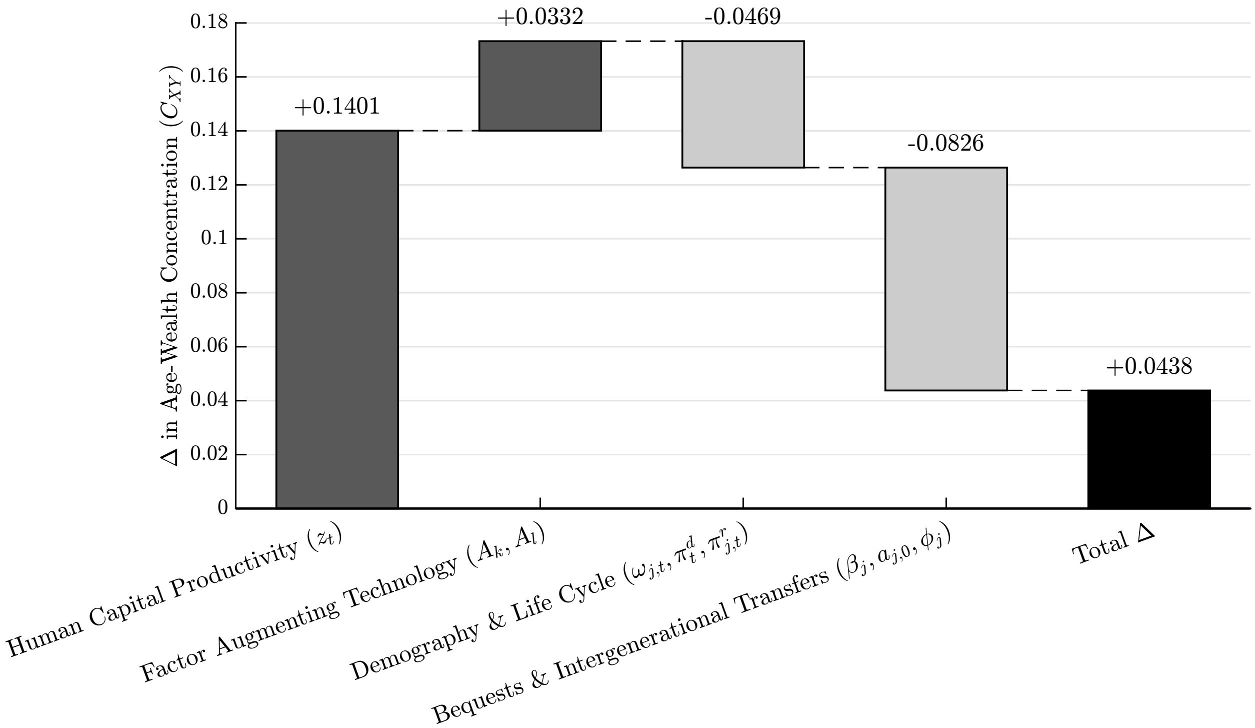


*Note:* This figure presents a Shapley value decomposition of the total historical shift in the macroeconomic age-wealth concentration curve ($C_{XY}$) between 1950 and 2010. The waterfall chart isolates the exact marginal contribution of four competing structural mechanisms within the general equilibrium transition path. Each step represents the average marginal effect of introducing the specified historical time-varying sequence into the model, evaluated across all $2^k$ counterfactual permutations. Positive values (dark gray bars) indicate mechanisms that drove an increase in intergenerational wealth inequality, while negative values (light gray bars) denote mechanisms that mitigated it.

inequality across the four economics mechanisms considered, while fully accounting for all possible general equilibrium interactions between them. The main results of the decomposition are displayed in Figure 8. For completeness, appendix Figures C.13 and C.14 also report results for the more traditional add-one-in and leave-one-out decompositions, respectively.

**Human Capital Productivity ($z_t$).** The decomposition in Figure 8 orders the contributions of each economic mechanism by their net impact on $C_{XY}$. The results show that the main driver of rising intergenerational wealth inequality in the post-war period is the increase in returns to human capital investment, $z_t$. The decomposition indicates that changes in $z_t$ alone increase the age-wealth concentration coefficient by 0.1401, over three times the total rise in wealth inequality during the sample period. In other words, increasing returns to human capital investment can account for more than the total rise in observed inequality.

Appendix Figure C.15 plots the model estimated path of $z_t$ along the economy's transition path. It shows that the returns to human capital investments rose sharply between the 1960s and 1970s, plateaued from the late 1980s through the early 2000s, and then declined through 2010. The path is reminiscent of the literature on skill-biased technological change and the closely related college wage premium, which exhibits similar dynamics over the same period.

The manner in which a rise in $z_t$ contributes to the rise in $C_{XY}$ is multifaceted. Facing higher returns to human capital investments, subsequent generations of young households optimally substitute their time from working to investing in human capital accumulation. Since human capital investments are costly in terms of foregone earnings, this reallocation suppresses early-life asset accumulation as young households run-down or delay savings in order to finance consumption in their youth. At the same time, the larger returns and increased investment in human capital leads to steeper lifecycle earnings profiles and inflates the peak of lifecycle earnings, driving increased asset accumulation later in life. On net then, the rise in $z_t$ contributes to an increase in $C_{XY}$ by both decreasing the physical savings of the young and increasing the income, and hence assets, of the old.

**Factor Augmenting Technologies and Relative Prices ($A_{k,t}, A_{l,t}$).** Factor-augmenting technological change lead to a 0.0332 increase in the concentration of wealth, equal to roughly 75% of the total rise within the model. Figure C.16 shows the model estimated dynamics of factor augmenting technologies for capital $A_{k,t}$ and labor $A_{l,t}$ along the equilibrium transition path. The figure shows that the labor-augmenting technology $A_{l,t}$ grew by a factor of three in the post-war period, while capital augmenting technology $A_{k,t}$ fell by half. All else equal, these changes in technology create a secular trend pushing up the returns to efficiency wages and pushing down the returns to physical capital. of course, the actual path of factor prices looks different from these trends as they also depend on households' endogenous labor supply and savings responses. Figure C.17 shows that on net, efficiency wages first rise and then fall, while Figure C.18 shows that returns on capital remain mostly flat.

The rise in labor-augmenting technology contributes to $C_{XY}$ through several channels. A secular rise in the demand for effective labor $A_{l,t}$ reinforces the incentive of young households to accumulate human capital, augmenting the forces discussed in the last subsection. Moreover, since the peak of effective labor supply (human capital) occurs late in life, the upward pressure on effective wages contributes more to the earnings of older and prime age workers, relative to the young who have just started to invest. As a result, wealth concentration increases as the young double down on human capital investments and the old receive even greater earnings from their accumulated human capital, boosting their ability to accumulate assets before retirement.

Decreases in the factor productivity of physical capital $A_{k,t}$ similarly contributes to rising wealth concentration. As with labor-augmenting technology, the fall in $A_{k,t}$–all else equal–incentivizes young workers to accumulate human versus physical capital. First, it puts downward pressure on the returns to physical capital relative to human capital. Second, the downward pressure on interest rates increases the net present value of future earnings, further reinforcing the incentive to invest in human versus physical capital. At the same time, reductions in $A_{k,t}$ can also decrease the wealth concentration by putting downward pressure on the returns to physical capital which are held predominantly by the old. However, in the quantitative model, these effects are relatively modest relative to the other forces, leading to an overall rise in wealth inequality. The results in Figures C.13 and C.14 highlight the isolated impact of each factor productivity by separately displaying the contribution $A_{k,t}$ and $A_{l,t}$ to the time-series of wealth inequality.

**Demographics and Life-Cycle Channels** $(\pi_t^d, \pi_{j,t}^r, \omega_{j,t})$ The joint impact of demographic change, represented by population aging ($\omega_{j,t}$), longevity ($\pi_t^d$), and the timing of retirement ($\pi^r_{j,t}$) dampened the rise in intergenerational inequality. Together, these forces reduced the concentration of wealth $C_{XY}$ by -0.0469. Figures C.19, C.20, and C.21 in the appendix display the aging, mortality, and retirement dynamics, respectively, employed in the counterfactual analysis.

The secular decline in mortality rates in the post-war period increased intergenerational wealth inequality. Intuitively, declines in mortality lengthen the period of retirement in which retirees must rely on their savings to finance consumption. Anticipating these changes, working households optimally increase their savings as they age and approach the retirement threshold. The result is increased asset holdings among older households, exacerbating the intergenerational concentration of wealth.

This effect is offset by the other demographic changes which push the opposite direction. First, the aging of the baby boom generation–readily evident in C.19–reduces the concentration of wealth by dispersing the aggregate capital stock across a broader demographic base of households. Second, the delayed age of retirement among subsequent cohorts in the latter half of the 20th century lengthens the period of working and compresses the duration of retirement. Later retirement pushes against the impact of declining mortality rates, leading to lower levels of optimal savings for older households which decreases wealth inequality. On the other hand, more years spent working increases the incentives for households to accumulate human capital, potentially exacerbating inequality. From the results in Figure C.13, we see the net impact of delayed retirement shrinks aggregate wealth inequality, suggesting the former effect dominates the latter. Taken together, Figure 8 shows that these changes had a net negative impact on the age-wealth concentration coefficient, suggesting the effect of aging and delayed retirement quantitatively dominate the impact of declining mortality.

**Bequests and Intergenerational Transfers ($\mathcal{F}_t, \beta_t, \phi_t$)** Changes in bequests, transfers, and residual savings motives reduced the concentration of wealth inequality by -0.0826. Of the four channels considered, these forces had the largest net negative impact on the age-wealth concentration coefficient. Together, these parameters control the initial asset holdings of new cohorts and the incentive they have to accumulate assets over their lifecycle.

As the data in Figure shows, there has been a steep secular rise in the initial wealth holdings of newly entering cohorts of 20-year-olds. Between 1950 and 2010, the average wealth of these young cohorts grew by nearly 50%. Economically, changes in this initial condition represents the impact of early-life transfers and inheritances received from older generations. Consistent with these changes, the model estimates an accompanying rise in the bequest motive $\phi_t$ of older households over the same period (see Table D.7). The larger wealth endowments received by young workers unambiguously lowers the age-wealth concentration ratio. As Figure C.13 show, changes in these initial conditions alone results in a consistent 0.05 reduction in the cross-age concentration of wealth throughout the sample period.

Finally, changes in residual savings motives captured by cohort specific shifts in the discount factor $\beta$ reveal a non-uniform impact on the rise in the cross-age concentration of wealth. Figure plots the model implied estimates of the discount factor across cohorts. It shows that the discount rate was relatively high for cohorts born between the 1920s and 1950, declined sharply during the 1960s and 1970s, and recovered strongly from the 1980s onward. In other words, the model suggests there were significant changes in the savings behavior of the middle cohorts which not directly captured by our other model mechanisms. Unsurprisingly, the impact of this cross-cohort heterogeneity on the aggregate intergenerational concentration of wealth is non-linear. As the add-one-in counterfactual time paths in Figure C.13 show, changes in the discount factor increase the concentration coefficient in the 1960s and 1970s, when the earlier cohorts with high discount factors reach prime age, and then shrink it at the end of the century when the lower discount factor cohorts from the 1960s and 1970s reach prime age. The net effect of these changes is relative modest however for most of the sample period, with the exception of the post-2000s. Altogether, the result suggests that other unmodeled features of household wealth accumulation behavior–such as changes in family structure, precautionary savings, taxation and social norms–may

Table 1: Intergenerational Welfare: Consumption Equivalent Variation

| Birth-Cohort | Total Shift | Decomposition by Mechanism | | | |
|---|---|---|---|---|---|
| | | Human Cap. ($z_t$) | Factor Tech. ($A_k, A_l$) | Demography ($\omega, \pi^d, \pi^r$) | Bequests ($a_{j,0}$) |
| 1930s | \$0 | \$0 | \$0 | \$0 | \$0 |
| 1940s | +\$22,801 | +\$10,448 | +\$10,442 | +\$1,135 | +\$776 |
| 1950s | +\$35,888 | +\$23,970 | +\$15,369 | -\$5,138 | +\$1,687 |
| 1960s | +\$25,687 | +\$27,506 | +\$9,252 | -\$12,712 | +\$1,641 |
| 1970s | +\$6,781 | +\$19,987 | +\$1,094 | -\$13,070 | -\$1,229 |
| 1980s | -\$9,245 | +\$10,000 | -\$6,953 | -\$13,548 | +\$1,255 |
| 1990s | -\$23,576 | -\$3,602 | -\$7,890 | -\$13,036 | +\$952 |

*Notes:* This table reports the intergenerational welfare shifts expressed as the annualized dollar Consumption Equivalent Variation (CEV). Values represent the annual dollar amount (2022 USD) that would need to be added to a household's consumption throughout a completely stationary 1950s baseline economy to make them indifferent between living in that stagnant economy versus the realized historical economy. The reported Total Shift encapsulates the total annualized premium experienced by subsequent cohorts due to changing macroeconomic conditions. The remaining columns utilize an exact Shapley value decomposition to allocate this dollar premium across the four fundamental mechanisms.

still be important contributors to the dynamics of wealth inequality.

## 5.2 Consumption-Equivalent Welfare

The preceding decomposition characterizes how the four mechanisms reshaped the distribution of wealth across generations. A shift in age-wealth concentration is, on its own however, silent about welfare. Much of the interest in the post-war rise in intergenerational inequality stems from the presumption that it signals deteriorating prospects for successive cohorts of young households. But a steeper age-wealth profile driven by young households optimally investing in high-return human capital carries a different welfare interpretation than one driven by young households being priced out of asset accumulation. To recover the welfare content behind the distributional shift, we complement the concentration decomposition with a consumption-equivalent welfare analysis across cohorts.

To quantify the absolute welfare implications of the historical transition, we compute the consumption-equivalent variation (CEV) for each birth cohort. Specifically, we calculate the constant dollar supplement to consumption (in 2022 USD) that would make a household born in the 1930s indifferent between its own realized life cycle and that of a household born in a later decades, whilst experiencing their realized sequence of prices, technologies, and demographic changes. A positive value therefore indicates that the later cohort is better off than the 1930s benchmark. As in the concentration exercise, we allocate the total welfare shift across the four structural mechanisms using an exact Shapley value decomposition, Table 1 presents the results.

Relative to the 1930s baseline, welfare rises for the first two cohorts and peaks at +\$35,888 for households born in the 1950s, after which it declines steadily, falling to +\$6,781 for the 1970s cohort and turning negative for cohorts born in the 1980s (−\$9,245) and 1990s (−\$23,576). The mid-century cohorts captured the largest welfare gains of the transition, while the most recent cohorts we track are worse off, in absolute terms, than households born half a century earlier. That is, the same historical transition that concentrated wealth in the hands of the old also delivered its largest lifetime gains to the cohorts experiencing their human capital accumulation years during the post-war boom, and imposed welfare losses only on the cohorts entering after the boom had been exhausted.

The Shapley decomposition attributes this hump-shape primarily to human capital productivity and, secondarily, to factor-augmenting technology, with demography acting as a persistent offset. Rising human capital productivity ($z_t$) is the dominant source of welfare gains for nearly every cohort, contributing +\$23,970 for the 1950s cohort and peaking at +\$27,506 for the 1960s cohort before fading and turning slightly negative (−\$3,602) for the 1990s cohort. This sign reversal is the welfare counterpart of the late-sample collapse in $z_t$ documented in Figure C.15: the youngest cohort we track enters the labor force just as the returns to skill acquisition unwind, and is the first to derive no welfare benefit from the human-capital channel. Factor-augmenting technology $(A_k, A_l)$ contributes positively for the earlier cohorts, peaking at +\$15,369 for the 1950s cohort, but becomes a welfare drag for cohorts born from the 1980s onward (−\$6,953 and −\$7,890). This mirrors the general-equilibrium price channel of the concentration analysis: labor-augmenting technical change eventually depressed the wage index while raising the return to capital, transferring welfare toward the capital-rich, earlier-born cohorts and away from the labor-reliant cohorts entering later.

Demographic and life-cycle change ($\omega_{j,t}, \pi_t^d, \pi_{j,t}^r$) is the principal and most persistent drag on cohort welfare. After a small positive contribution for the 1940s cohort, it turns sharply negative for every cohort from the 1960s onward, as population aging, lengthening retirement horizons, and shifting retirement timing raise the lifetime cost of financing consumption. Bequests and initial endowments ($a_{j,0}$) play only a modest role throughout, ranging from −\$1,229 to +\$1,687.

Taken together, the welfare accounting shows that the cohorts who lived through the post-war surge in human capital productivity and labor-augmenting technology enjoyed large lifetime gains, whist subsequent cohorts bear the welfare cost of the transition.

# 6 Conclusion

Over the post-war period the United States experienced a substantial rise in wealth inequality between older and younger people. By developing a dynamic, quantitative OLG framework we answer the question: what explains this rise in intergenerational inequality? Our decomposition reveals the evolution of the age-wealth distribution is the consequence technological forces and demographic headwinds. The primary cause for increasing inequalty was a surge in the returns to human capital. Concurrently, rapid expansions in labor-augmenting technology fundamentally affected the relative rental rates of wages and capital, suppressing the aggregate labor share and systematically economic rents toward older, capital-holding cohorts. The mechanical dispersion of capital caused by the aging of the baby boom generation, combined with endogenous behavioral adjustments to delayed labor force exit, larger early-life transfers, and stronger bequest incentives served to mitigate yet greater intergenerational inequality.

# References


Acemoglu, D., Autor, D., Beirne, K., and Scott, A. (2026). Baby busts and growth booms: Demographic change and the macroeconomy. Working Paper 35401, National Bureau of Economic Research.

Acemoglu, D. and Restrepo, P. (2022). Tasks, automation, and the rise in U.S. wage inequality. *Econometrica*, 90(5):1973–2016.

Adermon, A., Lindahl, M., and Waldenström, D. (2018). Intergenerational wealth mobility and the role of inheritance: Evidence from multiple generations. *The Economic Journal*, 128(612):F482–F513.

Allen, T. and Arkolakis, C. (2014). Trade and the topography of the spatial economy. *The Quarterly Journal of Economics*, 129(3):1085–1140.

Alon, T., Cox, N., and Kim, M. (2026). Misallocation and the early career consequences of student debt. Working paper.

Antunes, A. and Ercolani, V. (2020). Intergenerational wealth inequality: the role of demographics. Working Paper w202009, Banco de Portugal, Economics and Research Department.

Auclert, A., Malmberg, H., Martenet, F., and Rognlie, M. (2021). Demographics, wealth, and global imbalances in the twenty-first century. NBER Working Paper 29161, National Bureau of Economic Research. Forthcoming, Review of Economic Studies.

Audoly, R., McGee, R., Ocampo-Diaz, S., and Paz-Pardo, G. (2025). A practitioner's note on the shapley-owen-shorrocks decomposition. *FRB of New York Staff Report*, (1163).

Auerbach, A. J. and Kotlikoff, L. J. (1987). *Dynamic Fiscal Policy*. Cambridge University Press, Cambridge.

Auten, G. and Splinter, D. (2024). Income inequality in the united states: Using tax data to measure long-term trends. *Journal of Political Economy*, 132(7):2179–2227.

Autor, D., Dorn, D., Katz, L. F., Patterson, C., and Van Reenen, J. (2020). The fall of the labor share and the rise of superstar firms. *The Quarterly journal of economics*, 135(2):645–709.

Bartscher, A. K., Kuhn, M., and Schularick, M. (2020a). The college wealth divide: Education and inequality in america, 1956–2016. *Federal Reserve Bank of St. Louis Review*, 102(1):19–49.

Bartscher, A. K., Kuhn, M., Schularick, M., and Steins, U. I. (2020b). Modigliani meets minsky: Inequality, debt, and financial fragility in america, 1950-2016. Staff Report No. 924, Federal Reserve Bank of New York.

Bauluz, L. and Meyer, T. (2025). The Wealth of Generations. Working Paper 2024/04, World Inequality Lab. Latest version June 12, 2025.

Becker, G. S. (1964). *Human Capital: A Theoretical and Empirical Analysis, with Special Reference to Education.* National Bureau of Economic Research, distributed by Columbia University Press, New York.

Becker, G. S. and Tomes, N. (1979). An equilibrium theory of the distribution of income and intergenerational mobility. *Journal of Political Economy*, 87(6):1153–1189.

Ben-Porath, Y. (1967). The production of human capital and the life cycle of earnings. *Journal of political economy*, 75(4, Part 1):352–365.

Benhabib, J., Bisin, A., and Luo, M. (2019). Wealth distribution and social mobility in the us: A quantitative approach. *American Economic Review*, 109(5):1623–47.

Bloom, D. E., Canning, D., and Graham, B. (2003). Longevity and life-cycle savings. *The Scandinavian Journal of Economics*, 105(3):319–338.

Blundell, R., French, E., and Tetlow, G. (2016). Retirement incentives and labor supply. In *Handbook of the economics of population aging*, volume 1, pages 457–566. Elsevier.

Boserup, S. H., Kopczuk, W., and Kreiner, C. T. (2016). The role of bequests in shaping wealth inequality: Evidence from Danish wealth records. *American Economic Review*, 106(5):656–661.

Card, D. (1999). The causal effect of education on earnings. In Ashenfelter, O. C. and Card, D., editors, *Handbook of Labor Economics*, volume 3A, chapter 30, pages 1801–1863. Elsevier, Amsterdam.

Carvalho, C., Ferrero, A., and Nechio, F. (2016). Demographics and real interest rates: Inspecting the mechanism. *European Economic Review*, 88:208–226.

Chetty, R. (2006). A new method of estimating risk aversion. *American Economic Review*, 96(5):1821–1834.

De Loecker, J., Eeckhout, J., and Unger, G. (2020). The rise of market power and the macroeconomic implications. *The Quarterly Journal of Economics*, 135(2):561–644.

De Nardi, M. (2004). Wealth inequality and intergenerational links. *The Review of Economic Studies*, 71(3):743–768.

De Nardi, M. and Fella, G. (2017). Saving and wealth inequality. *Review of Economic Dynamics*, 26:280–300.

De Nardi, M., French, E., and Jones, J. B. (2010). Why do the elderly save? the role of medical expenses. *Journal of Political Economy*, 118(1):39–75.

De Nardi, M. and Yang, F. (2014). Bequests and heterogeneity in retirement wealth. *European Economic Review*, 72:182–196.

Dettling, L. J. and Hsu, J. W. (2014). The state of young adults' balance sheets: Evidence from the survey of consumer finances. *Federal Reserve Bank of St. Louis Review*, 96(4):305–330.

Dinerstein, M., Megalokonomou, R., and Yannelis, C. (2022). Human capital depreciation and returns to experience. *American Economic Review*, 112(11):3725–3762.

Doepke, M. and Schneider, M. (2006). Inflation and the redistribution of nominal wealth. *Journal of Political Economy*, 114(6):1069–1097.

Eggertsson, G. B., Mehrotra, N. R., and Robbins, J. A. (2019). A model of secular stagnation: Theory and quantitative evaluation. *American Economic Journal: Macroeconomics*, 11(1):1–48.

Elsby, M. W., Hobijn, B., and Şahin, A. (2013). The decline of the us labor share. *Brookings Papers on Economic Activity*, 2013(2):1–52.

Fagereng, A., Gomez, M., Gouin-Bonenfant, É., Holm, M., Moll, B., and Natvik, G. (2025). Asset-price redistribution. *Journal of Political Economy*, 133(11):3494–3549.

Feiveson, L. and Sabelhaus, J. (2019). Lifecycle patterns of saving and wealth accumulation. Finance and Economics Discussion Series 2019-010, Board of Governors of the Federal Reserve System (U.S.).

Gagnon, E., Johannsen, B. K., and López-Salido, D. (2021). Understanding the new normal: The role of demographics. *IMF Economic Review*, 69(2):357–390.

Gale, W. G., Gelfond, H., Fichtner, J. J., and Harris, B. H. (2020). The wealth of generations, with special attention to the millennials. Technical Report 27123, National Bureau of Economic Research.

Gale, W. G. and Scholz, J. K. (1994). Intergenerational transfers and the accumulation of wealth. *Journal of Economic Perspectives*, 8(4):145–160.

Glover, A., Heathcote, J., Krueger, D., and Ríos-Rull, J.-V. (2020). Intergenerational redistribution in the great recession. *Journal of Political Economy*, 128(10):3730–3778.

Goldin, C. and Katz, L. F. (2008). *The Race between Education and Technology*. Belknap Press of Harvard University Press, Cambridge, MA.

Gomez, M. (2025). Wealth inequality and asset prices. *The Review of Economic Studies*, 92(6):3924–3967.

Greenwald, D. L., Leombroni, M., Lustig, H., and Van Nieuwerburgh, S. (2025). Wealth inequality with declining interest rates. NBER Working Paper 28613, National Bureau of Economic Research. December 31, 2025; first draft March 2021. Originally circulated as "Financial and Total Wealth Inequality with Declining Interest Rates".

Guvenen, F. and Kuruscu, B. (2012). Understanding the evolution of the U.S. wage distribution: A theoretical analysis. *Journal of the European Economic Association*, 10(3):482–517.

Guvenen, F., Kuruscu, B., and Ozkan, S. (2014). Taxation of human capital and wage inequality: A cross-country analysis. *The Review of Economic Studies*, 81(2):818–850.

Heathcote, J., Perri, F., and Violante, G. L. (2010). Unequal we stand: An empirical analysis of economic inequality in the united states, 1967–2006. *Review of Economic Dynamics*, 13(1):15–51. Special issue: Cross-Sectional Facts for Macroeconomists.

Heathcote, J., Storesletten, K., and Violante, G. L. (2017). Optimal tax progressivity: An analytical framework. *The Quarterly Journal of Economics*, 132(4):1693–1754.

Henderson, J. V., Squires, T., Storeygard, A., and Weil, D. (2018). The global distribution of economic activity: nature, history, and the role of trade. *The Quarterly Journal of Economics*, 133(1):357–406.

Hendricks, L. and Schoellman, T. (2014). Student abilities during the expansion of US education. *Journal of Monetary Economics*, 63:19–36.

Hubmer, J., Krusell, P., and Smith, Jr., A. A. (2021). Sources of US wealth inequality: Past, present, and future. In Eichenbaum, M. and Hurst, E., editors, *NBER Macroeconomics Annual 2020, Volume 35*, volume 35, pages 391–455. University of Chicago Press.

Huggett, M. and Kaplan, G. (2016). How large is the stock component of human capital? *Review of Economic Dynamics*, 22:21–51.

Huggett, M., Ventura, G., and Yaron, A. (2011). Sources of lifetime inequality. *American Economic Review*, 101(7):2923–2954.

Jordà, Ò., Schularick, M., and Taylor, A. M. (2017). Macrofinancial History and the New Business Cycle Facts. *NBER macroeconomics annual*, 31(1):213–263.

Karabarbounis, L. and Neiman, B. (2014). The global decline of the labor share. *The Quarterly journal of economics*, 129(1):61–103.

Katz, L. F. and Murphy, K. M. (1992). Changes in relative wages, 1963–1987: Supply and demand factors. *The Quarterly Journal of Economics*, 107(1):35–78.

Kennickell, A. B. and Woodburn, R. L. (1999). Consistent weight design for the 1989, 1992 and 1995 scfs, and the distribution of wealth. *Review of Income and Wealth*, 45(2):193–215.

Knoblach, M. and Stöckl, F. (2020). What determines the elasticity of substitution between capital and labor? a literature review. *Journal of Economic Surveys*, 34(4):847–875.

Kotlikoff, L. J. and Summers, L. H. (1981). The role of intergenerational transfers in aggregate capital accumulation. *Journal of Political Economy*, 89(4):706–732.

Krueger, D. and Ludwig, A. (2007). On the consequences of demographic change for rates of returns to capital, and the distribution of wealth and welfare. *Journal of Monetary Economics*, 54(1):49–87.

Kuhn, M., Schularick, M., and Steins, U. I. (2020). Income and wealth inequality in america, 1949–2016. *Journal of Political Economy*, 128(9):3469–3519.

McKernan, S.-M., Ratcliffe, C. E., Steuerle, C. E., and Zhang, S. (2014). Impact of the great recession and beyond: Disparities in wealth building by generation and race. Working paper, The Urban Institute.

Mian, A. R., Straub, L., and Sufi, A. (2021). What explains the decline in r*? rising income inequality versus demographic shifts. *Rising Income Inequality Versus Demographic Shifts (September 22, 2021). University of Chicago, Becker Friedman Institute for Economics Working Paper*, (2021-104).

Mincer, J. (1974). *Schooling, Experience, and Earnings.* National Bureau of Economic Research, distributed by Columbia University Press, New York.

Modigliani, F. (1986). Life cycle, individual thrift, and the wealth of nations. *American Economic Review*, 76(3):297–313. Nobel Memorial Lecture.

Modigliani, F. (1988). The role of intergenerational transfers and life cycle saving in the accumulation of wealth. *Journal of Economic Perspectives*, 2(2):15–40.

Moll, B., Rachel, L., and Restrepo, P. (2022). Uneven growth: Automation's impact on income and wealth inequality. *Econometrica*, 90(6):2645–2683.

Munnell, A. H. (2025). Will the average retirement age keep rising? Issue in Brief 25-8, Center for Retirement Research at Boston College, Chestnut Hill, MA.

Nekoei, A. and Seim, D. (2023). How do inheritances shape wealth inequality? theory and evidence from Sweden. *The Review of Economic Studies*, 90(1):463–498.

Piketty, T. and Zucman, G. (2014). Capital is back: Wealth-income ratios in rich countries 1700–2010. *The Quarterly Journal of Economics*, 129(3):1255–1310.

Piketty, T. and Zucman, G. (2015). Wealth and inheritance in the long run. In *Handbook of income distribution*, volume 2, pages 1303–1368. Elsevier.

Poterba, J. M. (2001). Demographic structure and asset returns. *The Review of Economics and Statistics*, 83(4):565–584.

Restuccia, D. and Vandenbroucke, G. (2013). The evolution of education: A macroeconomic analysis. *International Economic Review*, 54(3):915–936.

Sabelhaus, J. and Volz, A. H. (2019). Are disappearing employer pensions contributing to rising wealth inequality? Federal Reserve Board FEDS Notes. Accessed: 2024-03-28.

Sabelhaus, J. and Volz, A. H. (2022). *Social Security Wealth, Inequality, and Lifecycle Saving*, pages 249–286. University of Chicago Press, Chicago.

Saez, E. and Zucman, G. (2016). Wealth inequality in the united states since 1913: Evidence from capitalized income tax data. *The Quarterly Journal of Economics*, 131(2):519–578.

Saez, E. and Zucman, G. (2020). The rise of income and wealth inequality in america: Evidence from distributional macroeconomic accounts. *Journal of Economic Perspectives*, 34(4):3–26.

Sastre, M. and Trannoy, A. (2002). Shapley inequality decomposition by factor components: Some methodological issues. *Journal of Economics*, 77(Suppl 1):51–89.

Shepard, M. (2022). Hospital network competition and adverse selection: evidence from the massachusetts health insurance exchange. *American Economic Review*, 112(2):578–615.

Shorrocks, A. F. et al. (2013). Decomposition procedures for distributional analysis: a unified framework based on the shapley value. *Journal of Economic Inequality*, 11(1):99–126.

Stansbury, A. and Summers, L. H. (2020). The declining worker power hypothesis: An explanation for the recent evolution of the american economy. *Brookings Papers on Economic Activity*, 51(1):1–96.

Wong, A. (2021). Refinancing and the transmission of monetary policy to consumption. Working Paper 2021-57, Princeton University, Department of Economics.

# Appendices

## Contents

# A Empirical Appendix

## A.I Data: Construction & Variables

In this section, we outline the data we use in our empirical analysis, chiefly the SCF and the SCF+. We describe how our dataset is constructed and the additional variables we create before describing additional supplemental data sources.

**The SCF and SCF+** The two main sources of data that we use in the empirical analysis are the SCF and the SCF+. The SCF is a triennial and cross-sectional survey of US families that runs from 1989 to 2022. The survey contains information on household balance sheets, income, and demographic characteristics. The SCF+ is a dataset constructed by Kuhn et al. (2020). The dataset combines archival household surveys 1949 through 1983, and is harmonized and reweighted to be compatible with the SCF. We normalize all nominal values in the SCF and SCF+ to 2022 dollars using the Consumer Price Index for All Urban Consumers series from the St. Louis Federal Reserve.

The merged SCF and SCF+ dataset covers a wealth of different asset classes, including holdings of equities, private business holdings, real estate, and vehicles. Following the work of Sabelhaus and Volz (2022), we impute wealth held in Defined Benefits (DB) retirement accounts.[18] We do this in two steps. First, for the survey years from 1989 through 2022, we use the DB wealth imputations from Sabelhaus and Volz (2019, 2022).[19] Second, for the years between 1949 and 1983, we impute DB wealth imputations using the method described in Bauluz and Meyer (2025).[20] In appendix table D.1 we present summary statistics for our

[18]DB retirement accounts are accounts where the employer or sponsor promises a specific periodic payment or lumpsum payment upon retirement. DB accounts were very prevalent in the US in the first half of our sample, but has gradually been replaced by Defined Contribution (DC) retirement accounts. However, wealth from DB accounts are not included in the SCF or the SCF+.

[19]Sabelhaus and Volz (2019) impute DB pension wealth in the SCF by utilizing detailed survey data on respondents' pension participation, expected retirement income, and work history. They supplement this information with aggregate data from the Financial Accounts of the United States (FAUS) to ensure that the total DB wealth in the SCF aligns with macroeconomic totals. This approach involves scaling individual DB wealth estimates to match the aggregate DB liabilities reported in the FAUS.

[20]Following Bauluz and Meyer (2025), we impute DB pension wealth for the historical waves of the SCF+

final dataset where prices are normalized to 2022-dollars.

Throughout the paper, we use the term ’wealth’ to mean ’net worth’ and use the variable ‘NETWORTH’, which appears in the SCF and SCF+. Net worth is calculated as the sum of total household assets less total liabilities.[21] As with all aggregate statistics in this paper, we calculate the weighted share of net worth using the post-stratified weights (Kennickell and Woodburn (1999)) that make our sample representative of the US population.

**Macro History Database** The Macrohistory Database complied by Jordà et al. (2017) contains long-run macro-financial data for 18 advanced economies since 1870 observed on an annual basis. For this paper, this dataset's main advantage is the availability of annual rates of return on total wealth, which we use to discipline the exogenous macroeconomic environment.

**Demographic and Life-Cycle Data** We supplement the core datasets with three data sources which detail on the evolution of demographic and life-cycle trends. First, to construct the time-varying probability of retirement we utilize historical labor force participation rates drawn from the American Community Survey (ACS) and decennial Census microdata. Second, to measure the shifting effective retirement age, we rely on the historical series taken from Munnell (2025), maintained by the Center for Retirement Research (CRR). Finally, to quantify the expanding retirement duration, we use the Historical and Projected Period Life Tables published by the Social Security Administration (SSA). These data sources provide exogenous inputs into the model which capture the change in workers' life cycles.

by using the age-wealth distribution of pension assets in modern SCF waves (from Sabelhaus and Volz, 2019, 2022) and adjusting it downward based on changes in life expectancy.

[21] See table D.1 for a complete taxonomy of the types of assets and liabilities included in the SCF and SCF+.

## A.II Additional Empirical Results

### A.II.1 Wealth Holdings by Alternative Age Thresholds

The motivating result reported in Figure 1 Panel B combines the rise in mean wealth reported in Panel A with a rise in the population share of older households, which we report in Figure C.2b. Beginning in 1950, the proportion of households with a head under 50 years of age is 64%, and by 2022 this falls to 38%.

We find similar increases in the share of net worth held by relatively older households when we consider alternative age groups in figure (C.3). Overall since 1950, the share of assets went from roughly equitable to an 80% share for 50-years-and-over households in 2022 and liabilities went from an 80% share for 50-years-and-over to a 45% share in 2022. Figures (C.3a) and (C.3b) show the net wealth shares for 45-and-older versus under-45 households, and 55-and-older versus under-55 households, respectively, where we find the share of the older households increase by 12 percentage points for the 45-and-older households and 38 percentage points for 55-and-older. Additionally, figure (C.3c) breaks down wealth shares into three age groups, 65 and over, 35-64, and under 35. We find that that 65-and-older households experience the largest increase in net wealth share whilst 35-64 households experience the largest decrease. The evolution of wealth concentration by household heads' age also depends on the evolution of households' asset and liabilities. To study the contributions of both sides of the balance sheet we plot in figure (C.4) the share of assets and liabilities held by 50-years-and-older and under-50 households. We find both sides of the balance sheet contribute to increased wealth concentration in older households. Panel (C.4a) shows roughly the same pattern for assets as for wealth: increasing rapidly beginning in the 1980s, but unlike the dynamics of wealth, closer to equitable for earlier survey waves. Panel (C.4b) on the other hand show since the 1970s liabilities have become consistently more concentrated in under-50 households. Overall since 1950, the share of assets went from roughly equitable to an 80% share for 50-years-and-over households in 2022 and liabilities went from an 80% share for 50-years-and-over to a 45% share in 2022.

### A.II.2 Age-Wealth Concentration by Asset Classes

In this subsection, we analyze the individual components that make up net worth. At a high level, we find that the change in age-wealth inequality is driven by changes across the age distribution in the ownership of non-financial assets, real estate, and business equity, while there has been a smaller change in inequality in the ownership of financial assets, such as equities.

Table D.2 reports the age-concentration of assets and liabilities. Specifically, we report the concentration coefficients, calculated using equation (2), replacing the variable wealth with each balance sheet item. Columns (1)-(3) show the coefficient calculated by pooling survey waves for each decade, similarly to figure C.5. Column (4) show the percentage change in concentration coefficient between (1) the 1950s and (2) 1980s, and column (5) shows the percentage change between (2) 1980s and (3) 2010s. A positive percentage change in concentration coefficients appearing in columns (4) & (5), indicates the age distribution of a particular balance sheet item favors relatively older households whilst a negative percentage change means the distribution favors younger households compared to before.

We begin by analyzing the least granular components of the balance sheet, those being assets, liabilities and residual net worth. The first row shows that the age-wealth concentration coefficient corresponding to the curves in figure C.5. Consistent with earlier discussion, we find that the age-wealth concentration coefficient increases significantly by 60.6% from the 1950s and 1980s and only increases by 8.8% between the 1980s and 2010s. Breaking this result down into assets and liabilities, both show a significant increase in age-concentration during the 1950s to 1980s, rising by 59.3% and 31.8%, respectively. However, between the 1980s and the 2010s, while the age-concentration of assets only increased by 9.7%, the age-concentration of liabilities decreased by 46.5%. We next analyze individual balance sheet items, which make up assets and liabilities.

We distinguish between financial and non-financial assets. In the SCF, financial assets are defined as assets that represent claims on real assets, such as stocks, bonds, and money in transaction and retirement accounts, while non-financial assets contain other significant assets such as real estate and businesses. Table D.2 reveals that both financial and non-financial assets became more concentrated in older households between 1950s and 1980s. Between 1980s and 2010s however, younger households actually acquire a larger share of financial assets whilst non-financial assets continue to become more concentrated amongst older households. Between the 1950s and 1980s the 17.4% increase in financial assets' age-concentration is a consequence of increasing concentration across all asset types, whilst the decrease in age-concentration between the 1980s and 2010s by 2.7% is driven by stocks and transaction accounts which are the first and third highest weighted financial assets in households' portfolios (see appendix figure C.6). The age-concentration of non-financial assets increases substantially by 79.9% between the 1950s and 1980s due to a rise in concentration across all non-financial assets, but particularly by business equity, which saw a rise of 129.2%. Between the 1980s and 2010s, non-financial assets' age-concentration continued to rise strongly by 10.5%, this time driven by primary residence and other real estate, which rose by 12.4% and 6.9% respectively. Given the rise in age-concentration of non-financial assets, it is important to note their importance for households' portfolios.[22]

Finally, turning our attention to individual liabilities, housing debt stands out as the largest component of liabilities, which saw significant increases in age-concentration; 24.7% between the 1950s and 1980s and 57.5% between the 1980s and 2010s (see C.7 for households' liabilities share). Personal debt stands out as the only large liability on household balance sheets which became less concentrated amongst older households: its age-concentration fell by 95% between the 1980s and 2010s.

To summarize, the change in the aggregate age-wealth concentration masks significant

[22]Appendix figure C.8 shows households' portfolio allocation in non-financial and financial assets over time, where most of households' assets are non-financial and this is particularly true for younger households. Figure C.9 provides a breakdown of non-financial assets which reveals that primary residence and business equity are the largest component's of household's portfolio allocation in non-financial assets.

heterogeneity across households' individual balance sheet items. Specifically, we find that the increased age-wealth concentration is primarily driven by non-financial assets, particularly business equity and real estate, which make up a significant component of households' portfolios. Financial assets' age-concentration also increased, but only between the 1950s and 1980s and decreased thereafter. Finally, liabilities are also more concentrated amongst older households, except for personal debt.

### A.II.3 Steepening Life Cycle Earnings Profiles

In this section, we document the significant steepening of life-cycle earnings trajectories over the post-war period. While aggregate data suggests a general increase in the returns to experience, this trend is almost entirely driven by college-educated households.

Figure (C.10) illustrates the evolution of mean labor income over the life cycle for four distinct generations: the Silent Generation (born between 1928-1945), Baby Boomers (1946-1964), Gen X (1965-1980), and Millennials (1981-1996). We partition the sample into two groups: households whose head has some college education (C.10b), and households for whom the head has none (C.10b). The rate of income appreciation during the first two decades of the career has accelerated sharply for college households. By age 40, the Gen X college-educated cohort have mean income levels significantly higher than those of the Silent Generation at the same stage of life, representing an expansion in career-peak earnings. At the same time, early career earnings fell as Gen X and Millenials earn less than Baby Boomers and the Silent Generation in their 20s.

In contrast, panel (C.10c) demonstrates that for households without college education, life-cycle earnings profiles have remained remarkably static. The profiles for the Silent Generation, Baby Boomers, and Gen X in the non-college group nearly overlap, indicating no change in life cycle income trajectories for this group. These facts suggest that the structural drivers of intergenerational inequality are tied to mechanisms that enhance the productivity of human capital investment. The widening gap in the slope of these earnings profiles suggests a potential channel through which wealth becomes increasingly concentrated in older, more educated households later in their life cycle.

Figure C.11 plots the educational composition of young adults (aged 25–34) across the historical transition. The data reveals a profound shift on both the extensive and intensive margins of educational attainment. Not only has the share of individuals with no college experience steadily fallen, but among those entering the higher education system, there is an increasing tendancy toward time-intensive advanced degrees (Bachelor's, Master's, Professional, and Doctorates). An expansion in the upper tail of educational attainment is consistent the steepening earnings profiles observed in figure C.10. By allocating significantly more years to advanced skill acquisition, recent generations forego higher early-career earnings, depressing average earnings of 20- to 29-year olds, only to experience income growth as they deploy this enhanced human capital later during their prime working years.

# B Calibration Appendix

## B.I Simulated Method of moments

let $\tilde{x}^S \equiv \{\tilde{x}_1, \ldots, \tilde{x}_S\}$ be $S$ simulations of the model data. The minimization problem is characterized by average moments across simulations, where $\tilde{m}_k(\tilde{x}^S|\theta) := 1/S \sum_{s=1}^{S} m(\tilde{x}_s|\theta)$ is the average of the $k^{\text{th}}$ moment and $\tilde{m}(\tilde{x}^S|\theta) = [\tilde{m}_1(\tilde{x}^S|\theta), \ldots, \tilde{m}_K(\tilde{x}^S|\theta)]'$. Let $m_k(x)$ be the actual $k^{\text{th}}$ moment computed from the data, then for a weighting matrix $W$, the chosen parameters minimize the weighted average of moment error functions, that is

$$\hat{\theta}^{\text{SMM}} = \arg\min_{\theta} (\tilde{m}(\tilde{x}^S|\theta) - m(x))' W (\tilde{m}(\tilde{x}^S|\theta) - m(x)) \tag{B.1}$$

## B.II Exogenous Macroeconomic Returns

To capture the secular decline in global interest rates we construct a time-varying sequence of exogenous macroeconomic returns, $\{R_t\}$. We draw on the MacroHistory Database, which provides extensive historical data on the rate of return on total wealth from the 1890s through the 2010s. To align with the model's decadal periodicity, the annual real rates of return are not averaged, but rather compounded to form a gross cumulative return. Specifically, the decadal return $R_t$ is calculated as:

$$1 + R_t = \prod_{k=1}^{10} (1 + r_{t,k}) \tag{B.2}$$

where $r_{t,k}$ is the historical annual real rate of return in year $k$ of calendar decade $t$. This cumulative return is then fed exogenously into the household's dynamic programming problem. Because solving the transition path requires boundary conditions extending beyond the historical data, we assume the global interest rate reaches a new permanent steady state following our observation window. Consequently, $R_t$ is extended forward, fixing all future returns (from the 2020s onward) at the final 2010s value.

## B.III Labor Force Transitions and Retirement Probabilities

The model requires a transition matrix governing the probability that an active worker in age cohort $j$ during calendar decade $t$ permanently exits the labor force, denoted as $\pi^r_{j,t}$. To discipline this matrix, we utilize historical labor force participation (LFP) rates from the American Community Survey (ACS) and decennial Census microdata. Let $L_{j,t}$ represent the male labor force participation rate for age group $j$ in decade $t$. Assuming retirement is an absorbing state, the decadal probability of retirement conditional on currently working is derived from the net cohort flow out of the labor force:

$$\pi^r_{j,t} = \max \left\{ 0, 1 - \frac{L_{j+1,t+1}}{L_{j,t}} \right\} \tag{B.3}$$

## B.IV Conditional Retirement Mortality

A central mechanism of the model is the changing duration of the retirement phase, driven simultaneously by shifting retirement ages and rising terminal life expectancies. The model condenses this horizon into a single geometric decay parameter: the decadal probability of death conditional on being retired, $\pi_t^d$.

To construct this sequence, we merge two external datasets. First, we obtain the average effective retirement age for men, $RA_t$, from the Center for Retirement Research (CRR) at Boston College. Second, we utilize the historical and projected Period Life Tables from the Social Security Administration (SSA). For each calendar decade $t = 1890, \ldots, 2080$, we locate the exact SSA remaining life expectancy, $e_{RA_t,t}$, for a male of exact age $RA_t$. Because $RA_t$ is a non-integer, $e_{RA_t,t}$ is calculated via linear interpolation between the bounding integer ages in the SSA tables. The expected retirement horizon in model periods (decades) is simply $e_{RA_t,t}/10$. Because the model treats retirement as a perpetual state with a constant death probability, the geometric decadal probability of death is the inverse of the expected horizon:

$$\pi_t^d = \frac{10}{e_{RA_t,t}} \tag{B.4}$$

To satisfy the boundary conditions required to solve the transition path, $\pi_t^d$ is padded with the stationary 1962 values for all pre-history periods, and fixed at the projected 2024 values for all future stationary periods. Furthermore, consistent with the SCF's historical definition of the "household head," this calibration strictly utilizes male retirement ages and male life tables to prevent shifting female labor force participation from contaminating the structural human capital estimates.

## B.V Demographic Structure and Population Weights

To aggregate individual household choices into macroeconomic variables (e.g., aggregate capital $K_t$ and effective labor $L_t$) and to compute cross-sectional inequality metrics like the

Age-Wealth Concentration curve, the model requires the precise demographic mass of each age cohort in each decade, $\omega_{j,t}$.

These cross-sectional population weights are derived directly from the Survey of Consumer Finances (SCF) for the available survey decades spanning 1950 through the 2010s. For each decade, we sum the post-stratified survey weights of all households within each decadal age bin $j$. The weights are then normalized such that the total population mass in any given decade sums to unity:

$$\sum_{j} \omega_{j,t} = 1 \quad \forall t \tag{B.5}$$

Because the overlapping generations transition path evaluates cohorts living from 1890 to 2080, the demographic vectors must encompass the entire simulation window. To satisfy these boundary conditions, we assume a constant demographic steady state outside of our empirical observation window. We pad the transition path by fixing the pre-history population weights (1890 to 1940) at the 1950 distribution, and fixing the future population weights (2020 to 2080) at the final 2010s distribution.

## B.VI Exogenous General Equilibrium Wage Index

To empirically discipline the exogenous macroeconomic growth path of the general equilibrium wage, $\{W_t\}$, we construct a standardized wage index using historical microdata from the decennial Census and the American Community Survey (ACS). To isolate the "pure" rental price of an efficiency unit of labor, we identify a demographic cohort whose accumulated human capital is effectively at its baseline ($h \approx 1$) and whose ongoing human capital investment is strictly bounded near zero ($s \approx 0$). Specifically, we restrict our sample to male workers aged 20 to 29 whose highest educational attainment is exactly a high school diploma (12th grade equivalent). We also exclude individuals reporting zero or top-coded wage and salary income. To ensure that the observed earnings are not driven by endogenous, part-time labor supply choices, we further restrict the sample to Full-Time, Full-Year

(FTFY) workers. A significant challenge in utilizing long-run historical Census microdata is the structural break in how hours and weeks worked are reported over time. To guarantee that our sample selection criteria remain perfectly stationary across this break, we construct the FTFY indicator using strictly interval-based variables for the entire 1940–2010 sample. Workers are retained only if they fall into the 35–39 hours category (or higher) and the 40–47 weeks category (or higher). We compute a standardized real hourly proxy. Observed annual wage income is divided by a standard 2,000-hour work year and deflated to real constant dollars using the Consumer Price Index (CPI). Let $incwage_{i,t}$ be the nominal annual wage of individual $i$ in decade $t$, and let $cpi_t$ be the corresponding price deflator. The real hourly wage proxy is calculated as:

$$w_{i,t} = \frac{incwage_{i,t}}{2000} \times cpi_t \tag{B.6}$$

Finally, we apply cross-sectional person weights, to collapse the microdata into a decade-average, $\bar{w}_t$. Because the absolute initial level of the wage, $W_0$, is jointly identified within the Simulated Method of Moments (SMM) to scale the general equilibrium, we normalize the empirical time-series by its 1950 value. This yields the exogenous wage index sequence:

$$W_t^{index} = \frac{\bar{w}_t}{\bar{w}_{1950}} \tag{B.7}$$

We finally normalize the entire series by setting the 1950 index value to unity.

# C Appendix Figures

Figure C.1: The Age-Concentration Coefficient over Time

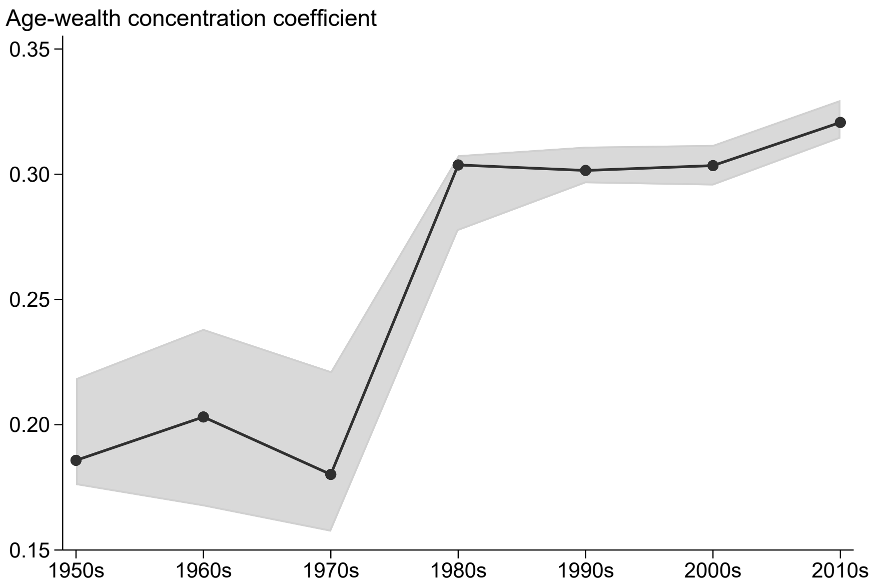


*Note:* This figure plots the age–wealth concentration coefficient by decade, from the 1950s to the 2010s. The coefficient equals one minus twice the area under the age–wealth concentration curve of Figure 2, the analogue of a Gini coefficient with households ranked from youngest to oldest; higher values indicate net worth held more disproportionately by older households. Each decade pools its constituent survey waves, with each wave rescaled to receive equal weight. The shaded region is the 90% confidence band, obtained from 999 bootstrap replicate weights as the 5th and 95th percentiles of the resulting replicate estimates. Data source: SCF+.

Figure C.2: Wealth and population shares for under and over 50

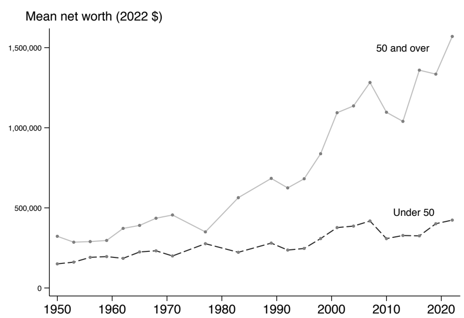


(a) Average wealth

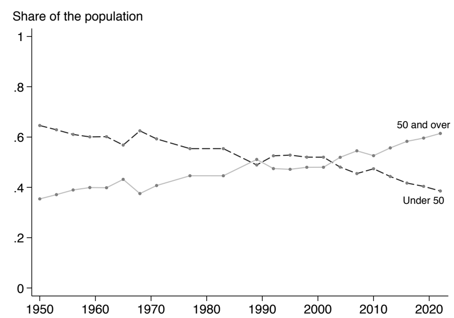


(b) Share of the population

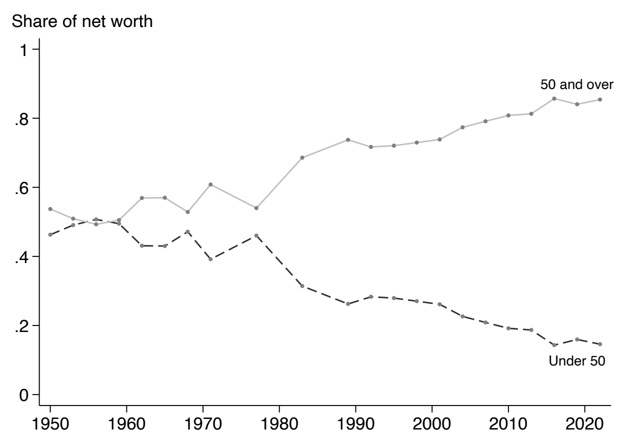


(c) Share of wealth

*Note:* These figures plot how the share of wealth, the share of the population, and average wealth for households under and over age 50 change over time. The data source is the SCF+. Panel A depicts the share of wealth, Panel B shows population shares, and Panel C shows average wealth. All data are weighted using the SCF+ adjusted survey weights.

Figure C.3: Wealth shares by Age Groups

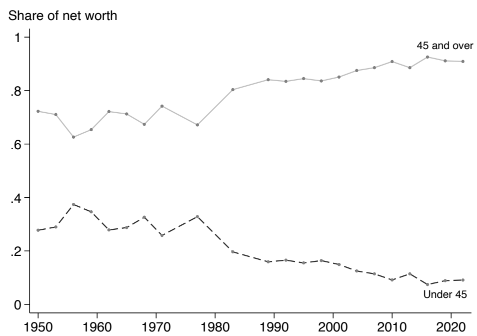


(a) Share of wealth under/over 45

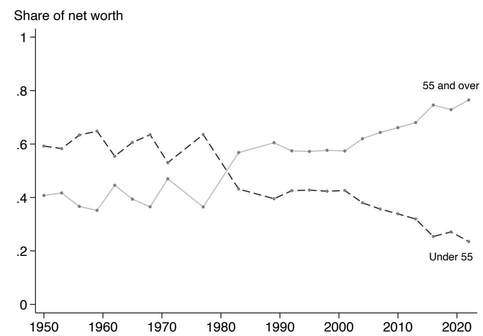


(b) Share of wealth under/over 55

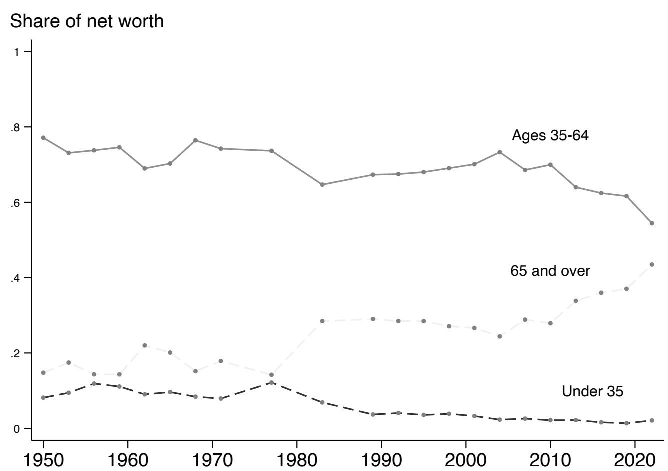


(c) Share of wealth

*Note:* These figures plot how the share of wealth changes over time. All data are weighted using the SCF+ adjusted survey weights. The top panels (left-to-right) show the wealth share for households under/over 45 years old and under/over 55 years old, respectively. The bottom panel shows the wealth share amoung three age groups, 65 and over, 35-64 and under 35. The data source is the SCF+.

Figure C.4: Asset and liability shares for under and over 50

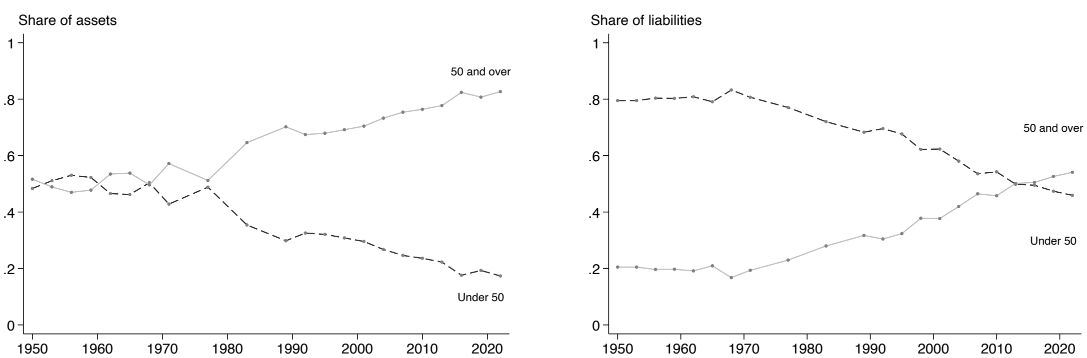


(a) Share of Assets

(b) Share of Liabilities

These figures plot how the share of assets (including the present value of defined benefit pension plans) and liabilities for under and over age 50 households change over time. The data source is the SCF+. All data are weighted using the SCF+ adjusted survey weights.

Figure C.5: Age-Wealth Distributions by Decade

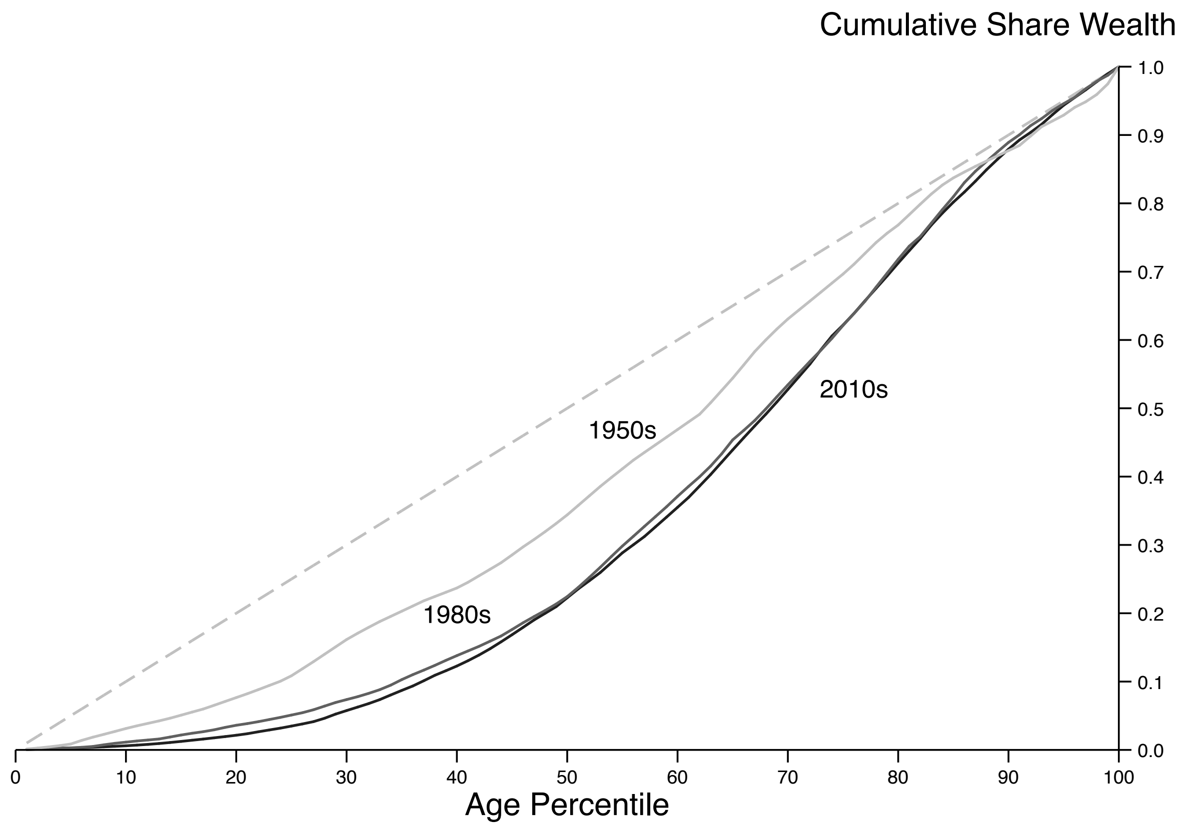


*Note:* This figure shows the concentration curve by age percentile during the 1950s and 2010s. The 1950s concentation curve constructed using the 1950, 1953, 1956, and 1959 SCF+ survey waves. The 2010s curve is constructed using the 2010, 2013, 2016, 2019, and 2022 SCF+ survey waves.

Figure C.6: Financial Assets Portfolio Share by Age Quartiles

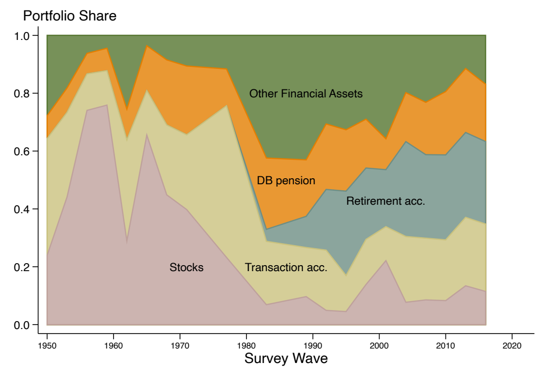


(a) 1st Quartile

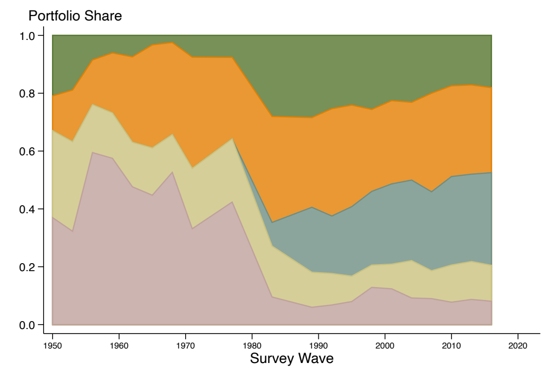


(b) 2nd Quartile

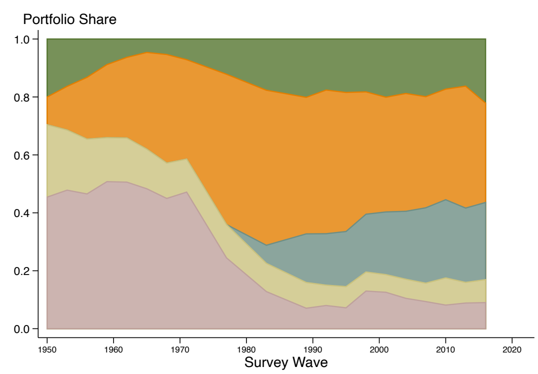


(c) 3rd Quartile

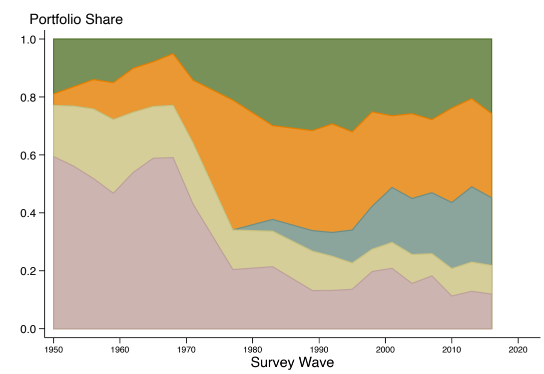


(d) 4th Quartile

*Note:* This figure shows a breakdown of mean portfolio allocation in financial assets classes for each quartile of the age distribution over the SCF+ survey waves. From top-to-bottom and left-to-right the panels show the portfolio allocation of the first quartile of the household head age distribution, followed by the second, third and fourth quartiles. All data is calculated using SCF+ adjusted survey weights.

Figure C.7: Liabilities Share by Age Quartiles

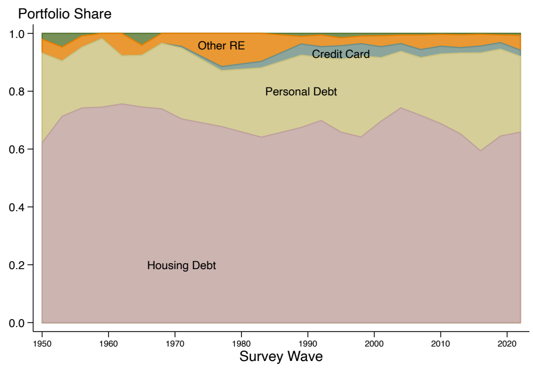


(a) 1st Quartile

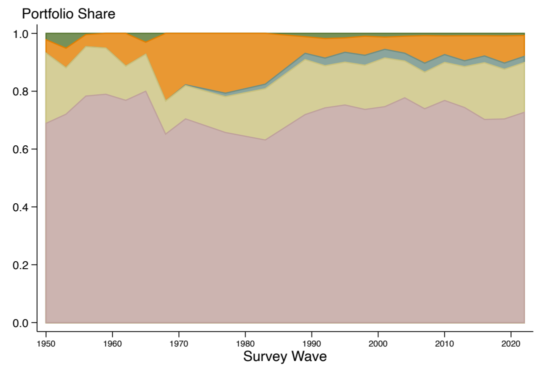


(b) 2nd Quartile

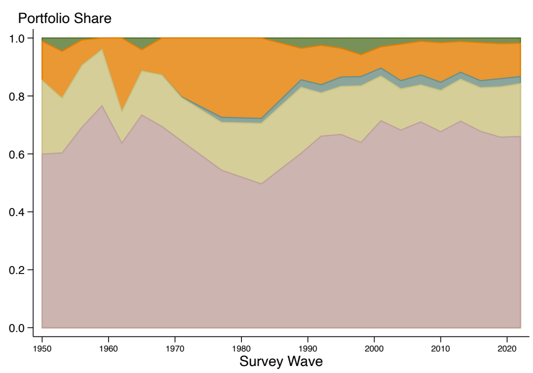


(c) 3rd Quartile

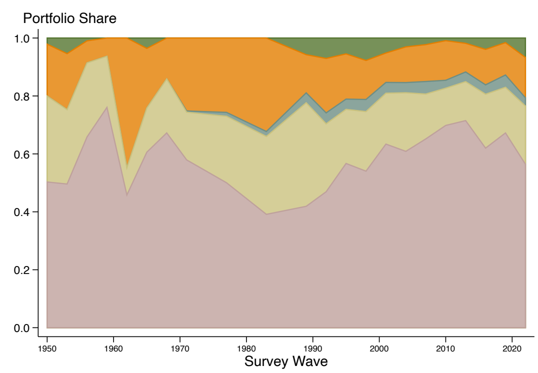


(d) 4th Quartile

*Note:* This figure shows a breakdown of mean liabilities for each quartile of the age distribution over the SCF+ survey waves. From top-to-bottom and left-to-right the panels show the liabilities composition of the first quartile of the household head age distribution, followed by the second, third and fourth quartiles. All data is calculated using SCF+ adjusted survey weights.

Figure C.8: Assets Portfolio Share over time by Age Quartiles

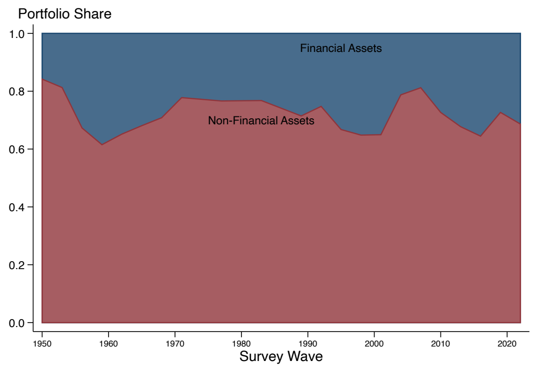


(a) 1st Quartile

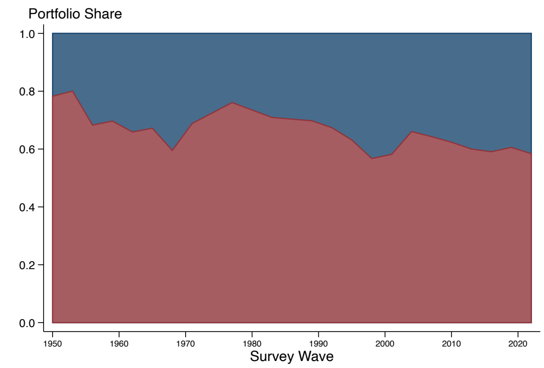


(b) 2nd Quartile

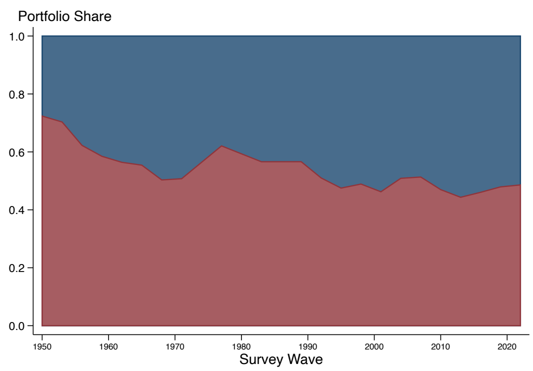


(c) 3rd Quartile

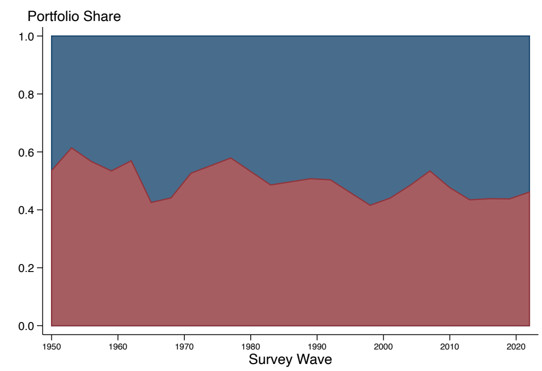


(d) 4th Quartile

*Note:* This figure shows the mean portfolio allocation in Financial and Non-financial assets for each quartile of the age distribution over the SCF+ survey waves. From top-to-bottom and left-to-right the panels show the portfolio allocation of the first quartile of the household head age distribution, followed by the second, third and fourth quartiles. All data is calculated using SCF+ adjusted survey weights.

Figure C.9: Non-Financial Assets Portfolio Share by Age Quartiles

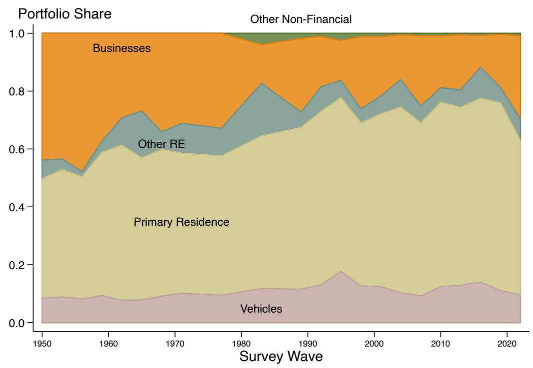


(a) 1st Quartile

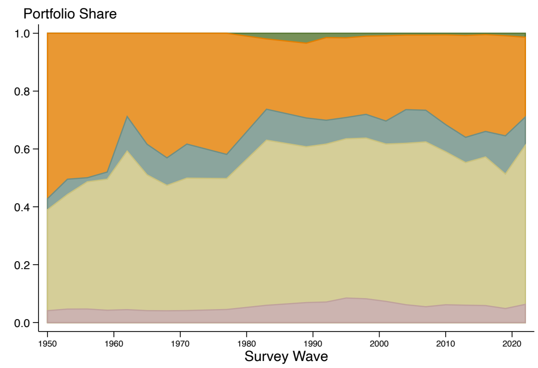


(b) 2nd Quartile

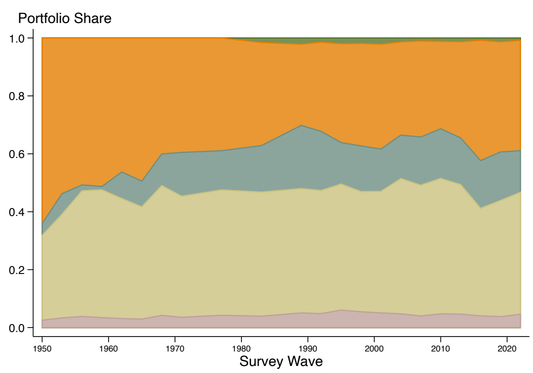


(c) 3rd Quartile

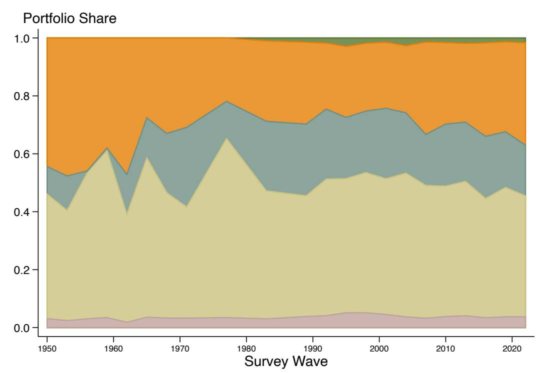


(d) 4th Quartile

*Note:* This figure shows a breakdown of mean portfolio allocation in Non-financial assets classes for each quartile of the age distribution over the SCF+ survey waves. From top-to-bottom and left-to-right the panels show the portfolio allocation of the first quartile of the household head age distribution, followed by the second, third and fourth quartiles. All data is calculated using SCF+ adjusted survey weights.

Figure C.10: Life-Cycle Income Across Generations

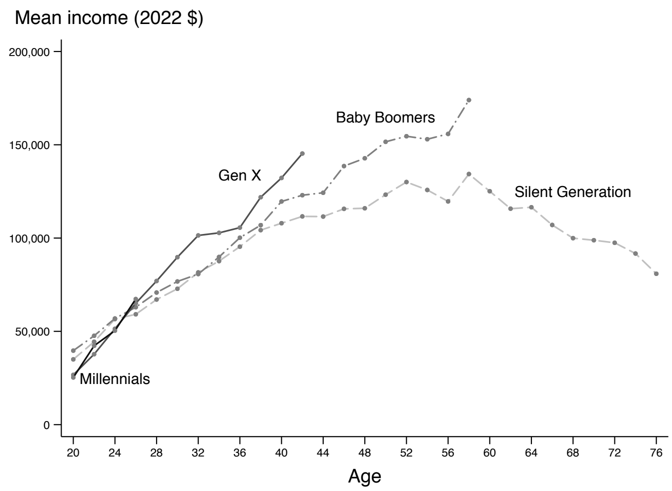


(a) All households

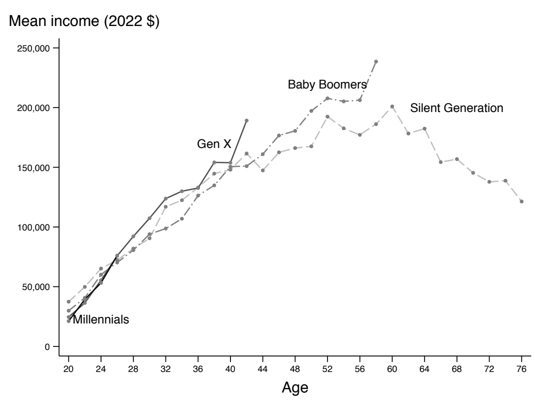


(b) College

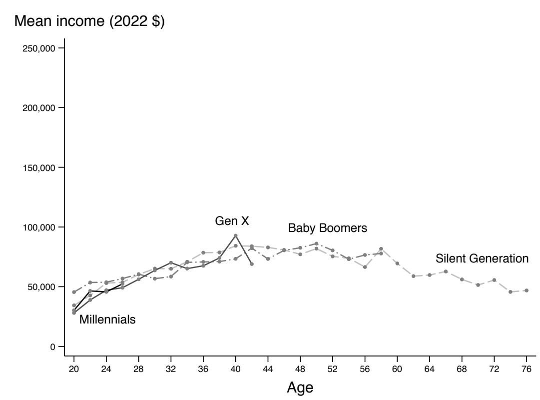


(c) Non-college

*Note:* Life-cycle income profiles by cohorts. Panel A shows all households, Panel B households with at least a 4-year degree, and Panel C no four-year degree.

Figure C.11: Educational Attainment by Adults Aged 25-34

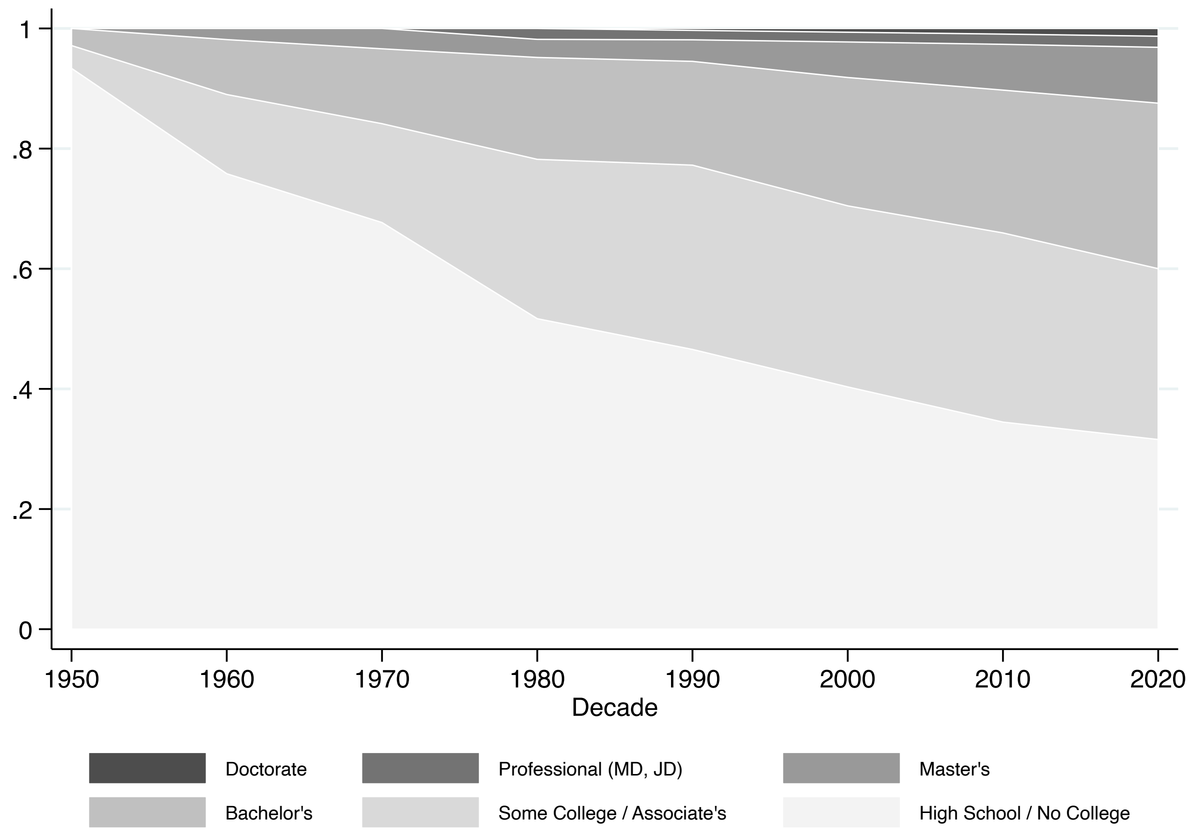


*Note:* This figure plots the educational composition of young adults (ages 25–34) by decade, using decennial Census and ACS data. The shaded regions denote the share of the population whose highest educational attainment falls into each respective category, capturing both the aggregate expansion of college attendance (extensive margin) and the shift toward highly time-intensive advanced degrees (intensive margin).

Figure C.12: Age-Wealth Concentration

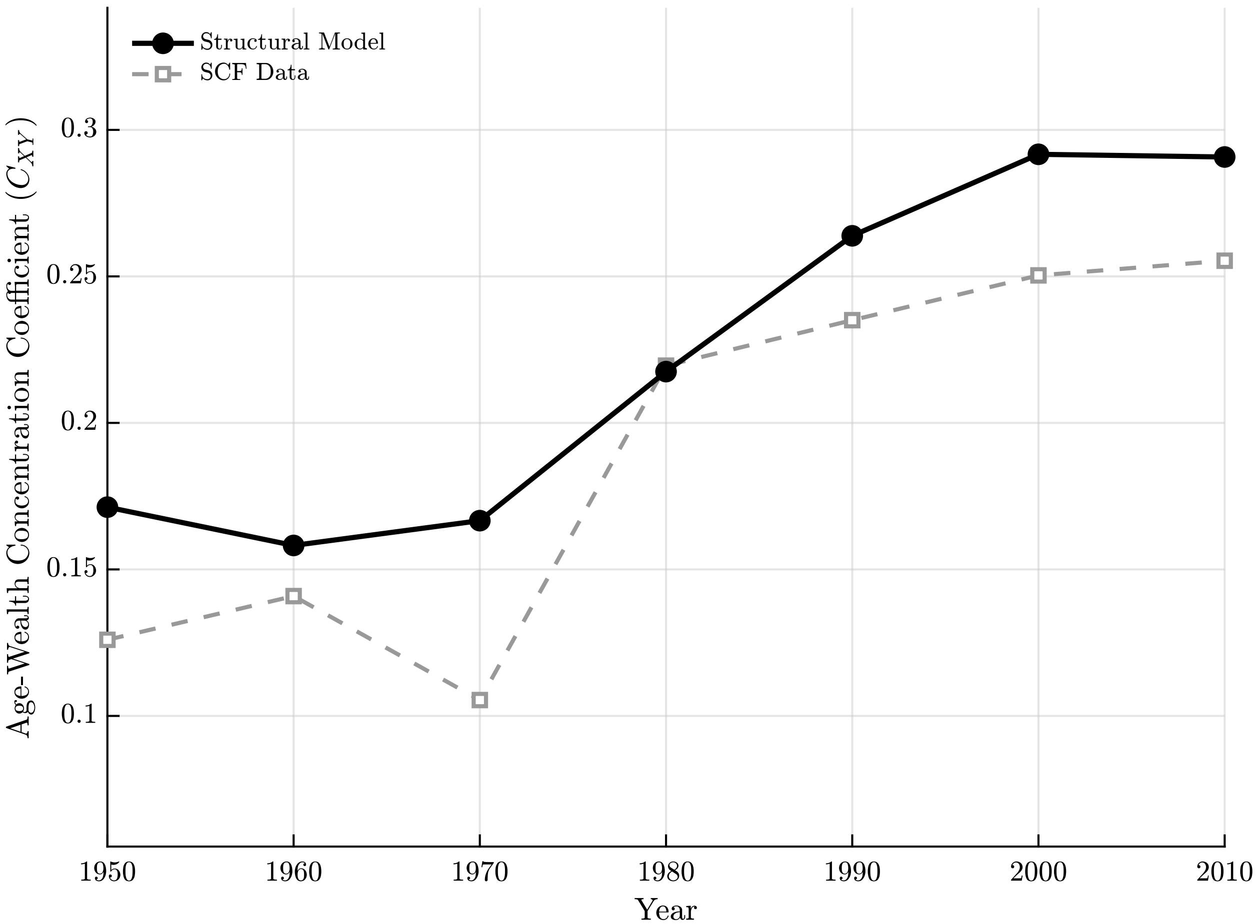


*Note:* This figure plots the time-series of the age-wealth concentration coefficient ($C_{XY}$) comparing the structural model (solid black) to empirical targets from the Survey of Consumer Finances (dashed grey). The $C_{XY}$ metric captures the degree to which wealth is concentrated across age-ranked percentiles of the population.

Figure C.13: Marginal Transition Dynamics (One-At-A-Time Counterfactuals)

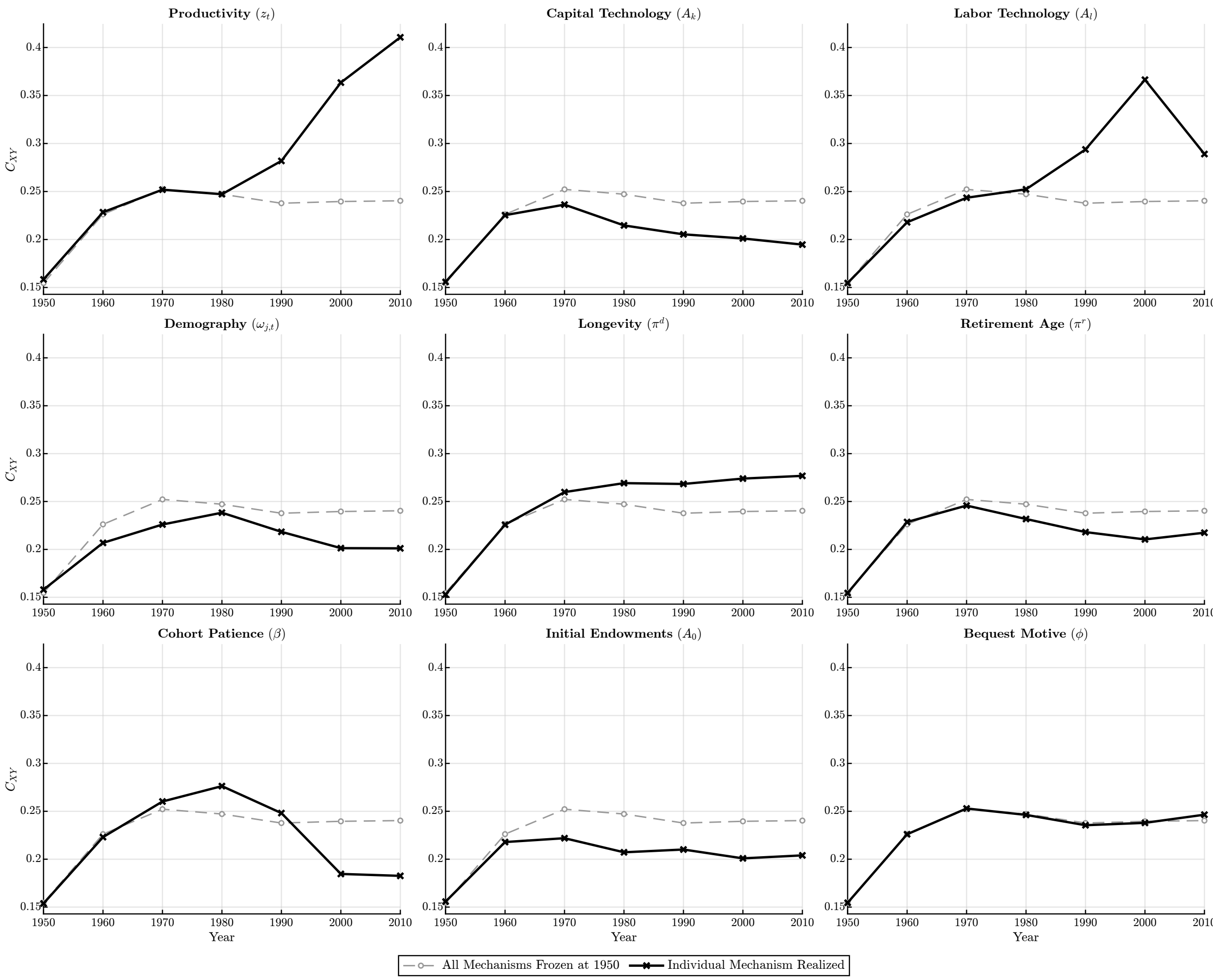


*Note:* This figure illustrates the "Add-One-In" marginal transition dynamics for the four structural mechanisms evaluated in general equilibrium. In each panel, the dashed gray line with circular markers represents the baseline counterfactual where all historical mechanisms are permanently frozen at their 1950 steady-state values. The solid black line isolates the macroeconomic effect of allowing only the specified mechanism to evolve along its historical trajectory, keeping the other mechanisms frozen.

Figure C.14: Marginal Transition Dynamics (Leave-One-Out Counterfactuals)

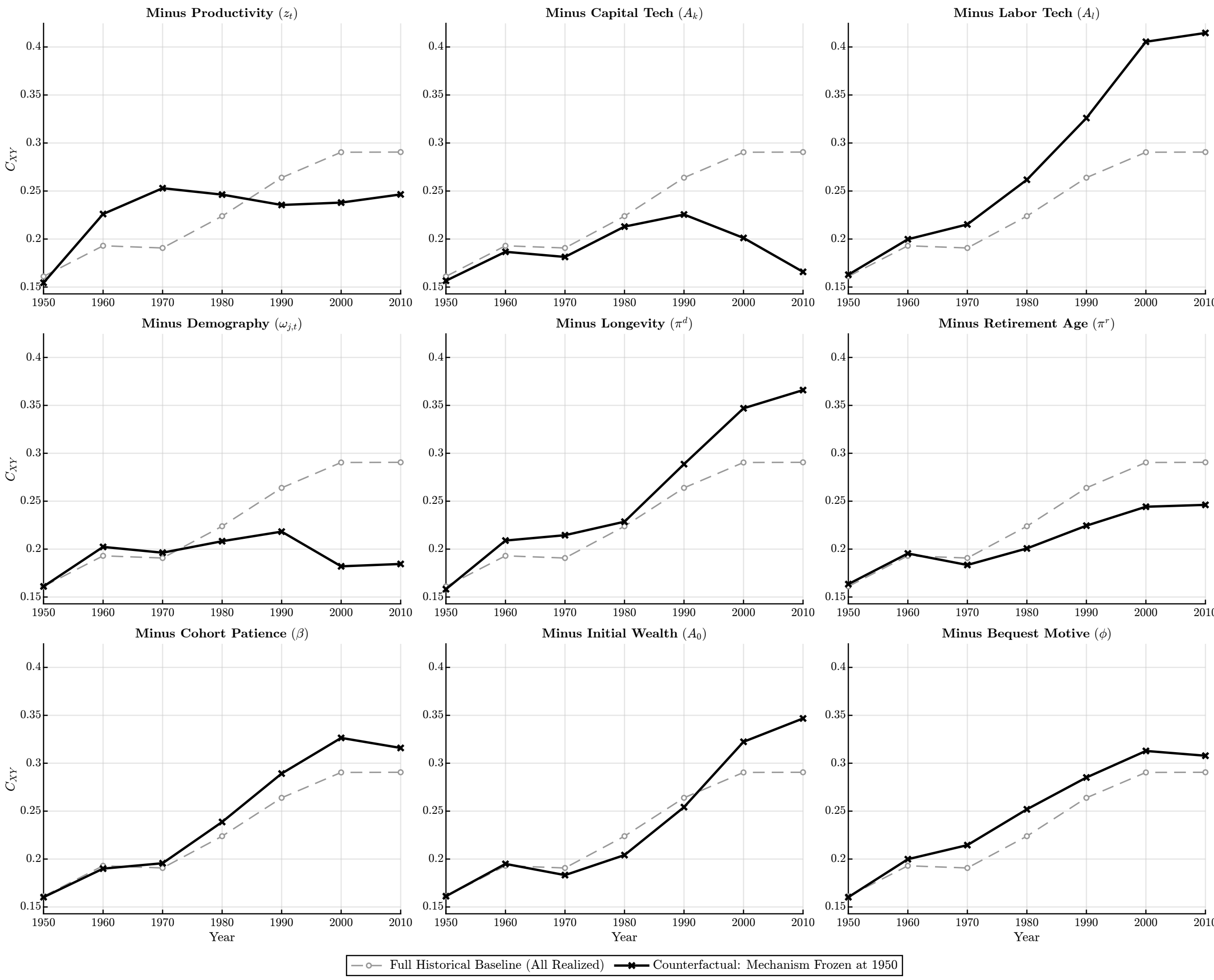


*Note:* This figure evaluates the marginal importance of each structural driver by comparing the full historical baseline (dashed grey line) against counterfactual scenarios where exactly one mechanism is removed (solid black line). In each panel, the "removed" mechanism is frozen at its calibrated 1950 level for the duration of the transition path, while all other historical drivers (productivity, technology, demographics, and longevity) follow their observed empirical trajectories.

Figure C.15: Estimated Path: Human Capital Productivity

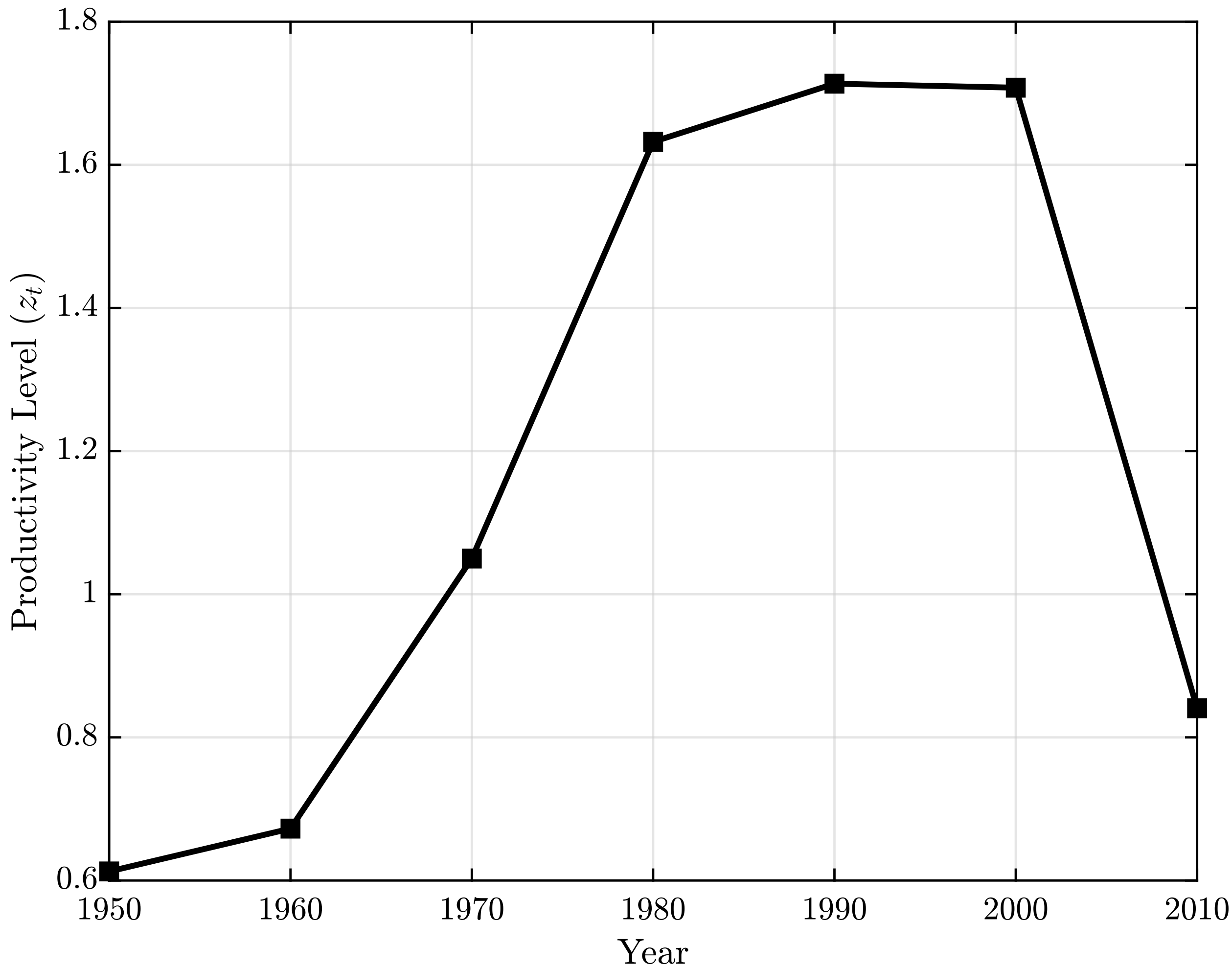


*Note:* This figure shows the estimated trajectory of human capital learning productivity ($z_t$), the core structural mechanism driving the model's intergenerational dynamics. This parameter dictates the efficiency with which households can transform foregone labor time ($s_{j,t}$) into future skill units ($h_{j+1,t}$).

Figure C.16: Implied Path of Human- and Physical- Capital Augmenting Technology

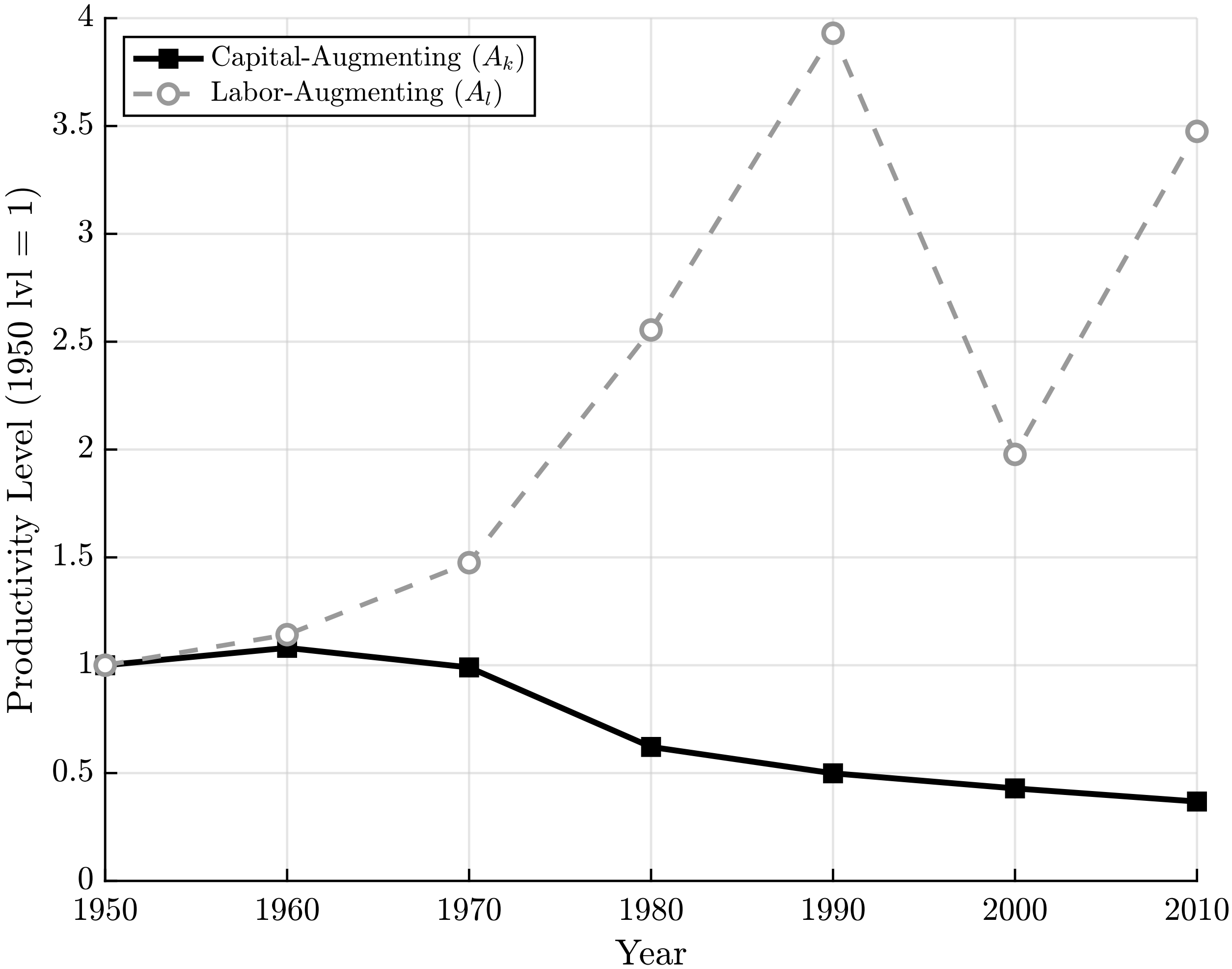


*Note:* This figure illustates the model-implied paths for capital-augmenting ($A_{k,t}$) and labor-augmenting ($A_{l,t}$) technology. They are recovered analytically as residuals from the representative firm's static First-Order Conditions (FOCs). Once the household optimization yields the aggregate supply of physical capital and effective human capital, and the sequences for the aggregate wage ($W_t$) and interest rate ($R_t$) are structurally identified, $A_{k,t}$ and $A_{l,t}$ represent the exact macroeconomic technology levels required to clear the factor markets in general equilibrium.

Figure C.17: Estimated Path: Rental Rate on Efficiency Units of Labor

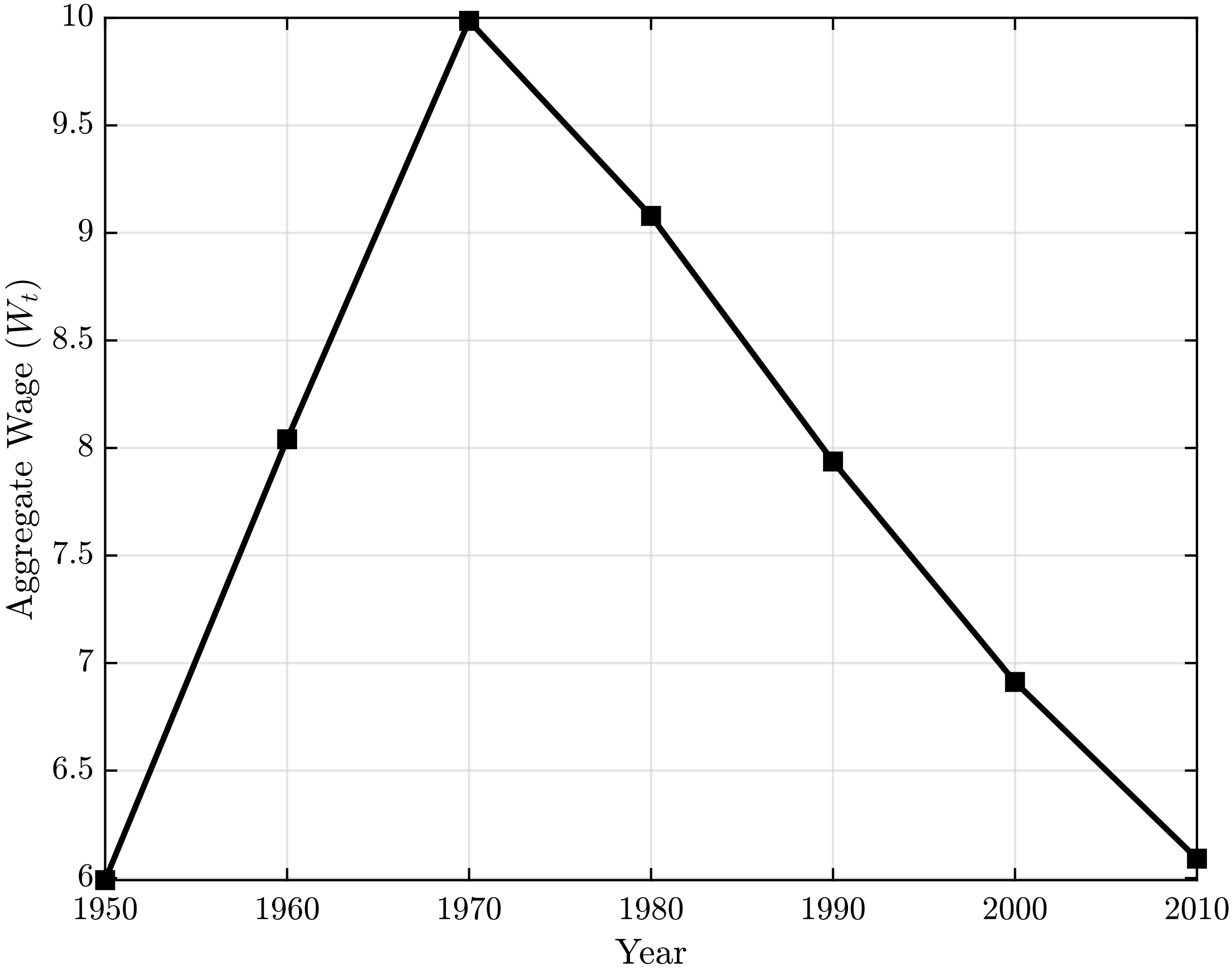


*Note:* This figure plots the estimated sequence for the unobservable general equilibrium wage ($W_t$). In this framework, $W_t$ represents the rental rate for a single *effective* unit of human capital, not the average aggregate earnings per worker.

Figure C.18: Interest Rate Path

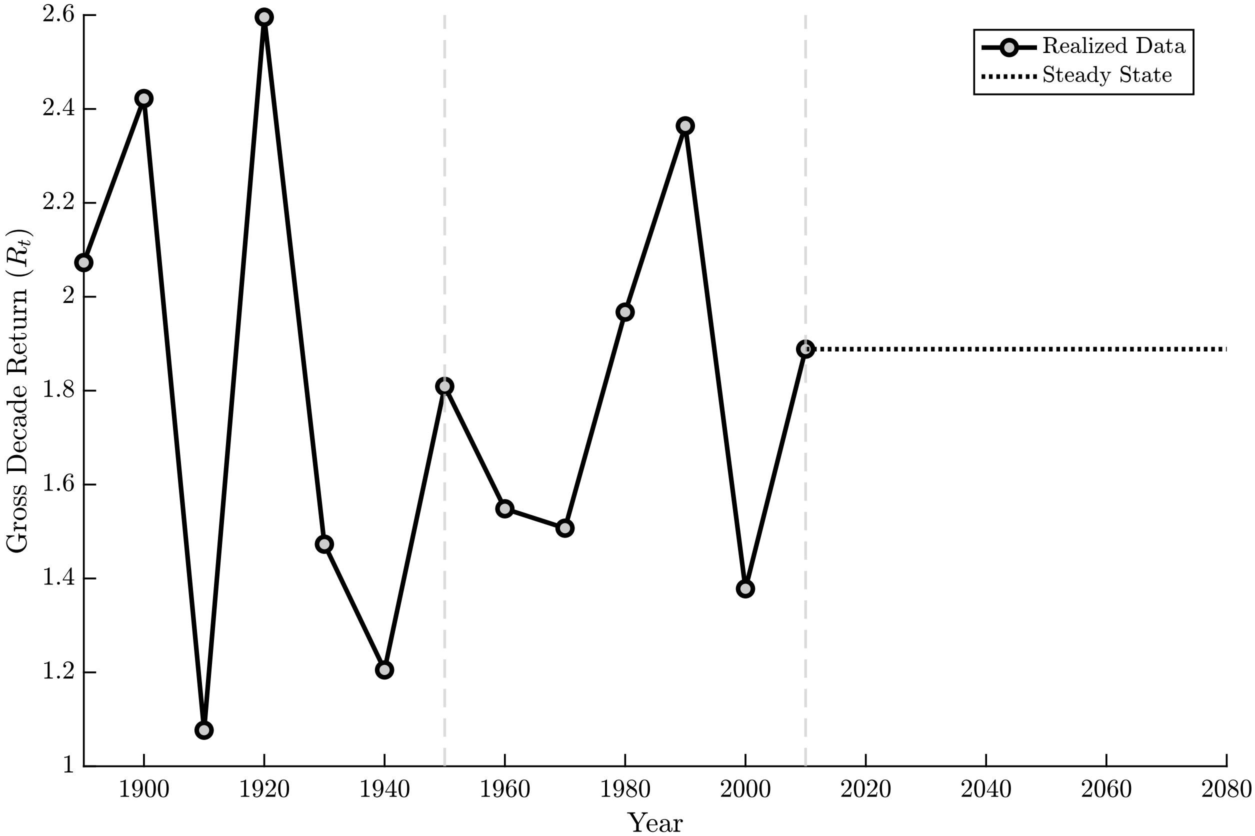


*Notes:* This table reports the intergenerational welfare shifts expressed as the Consumption Equivalent Variation (CEV). Values represent the constant 10-year period dollar amount (2022 USD) that would need to be gifted to the 1930s birth cohort to make them indifferent between their realized life cycle that experienced of subsequent generations. The reported "Total Shift" encapsulates the total per-period premium experienced by subsequent cohorts due to changing macroeconomic conditions. The remaining columns utilize an exact Shapley value decomposition.

Figure C.19: SCF+ IMPLIED DEMOGRAPHICS

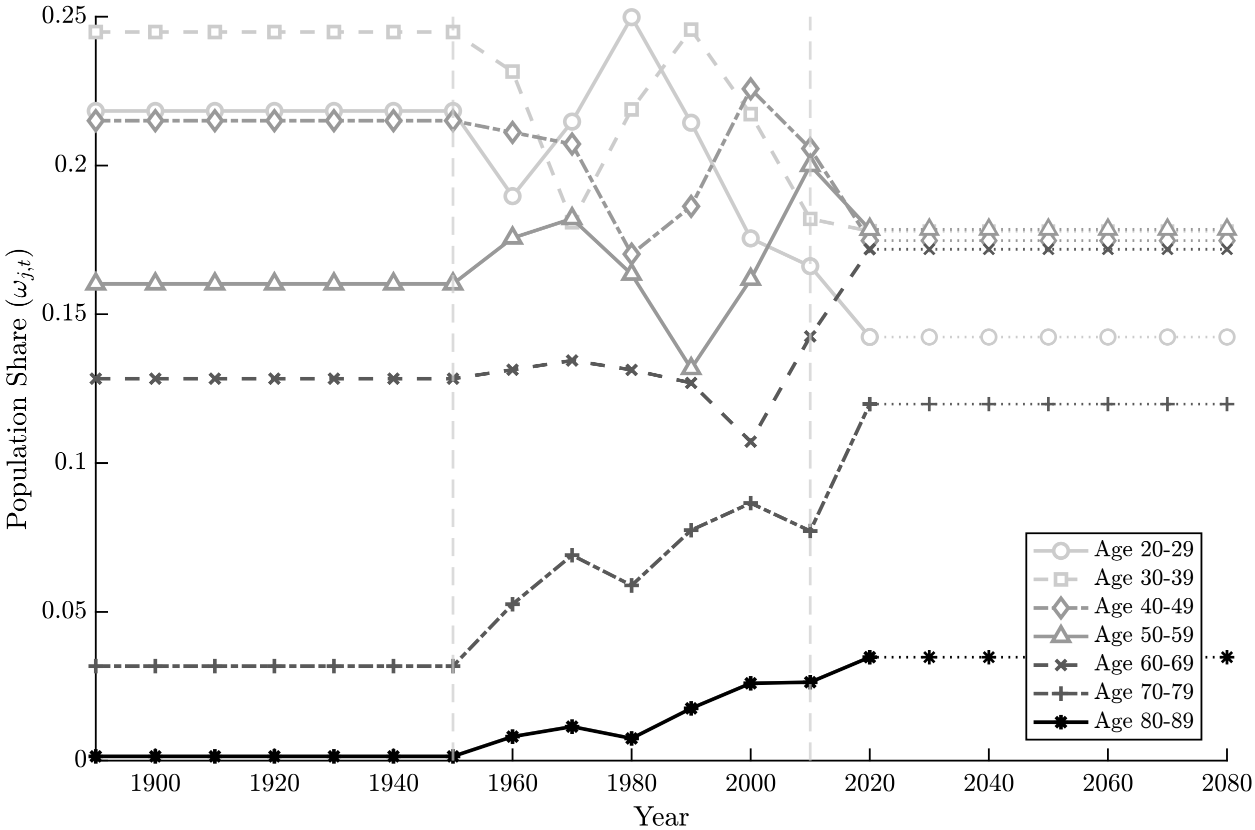


*Note:* This figure illustrates the evolution of macroeconomic population weights ($\Omega_{j,t}$) across the transition path. Data are derived from the Survey of Consumer Finances Plus' (SCF) post-stratified weights, aggregated by calendar decade and decadal age group. Solid lines represent realized historical data within the active calibration window, while dotted lines denote the projected terminal steady-state padding applied to cohorts post-2020. The selected cross-sections (e.g., ages 20–29, 40–49, 60–69, and 80–89) highlight the shifting age distribution, capturing the aging of the baby boom generation.

Figure C.20: Mortality Risk Conditional on Retired

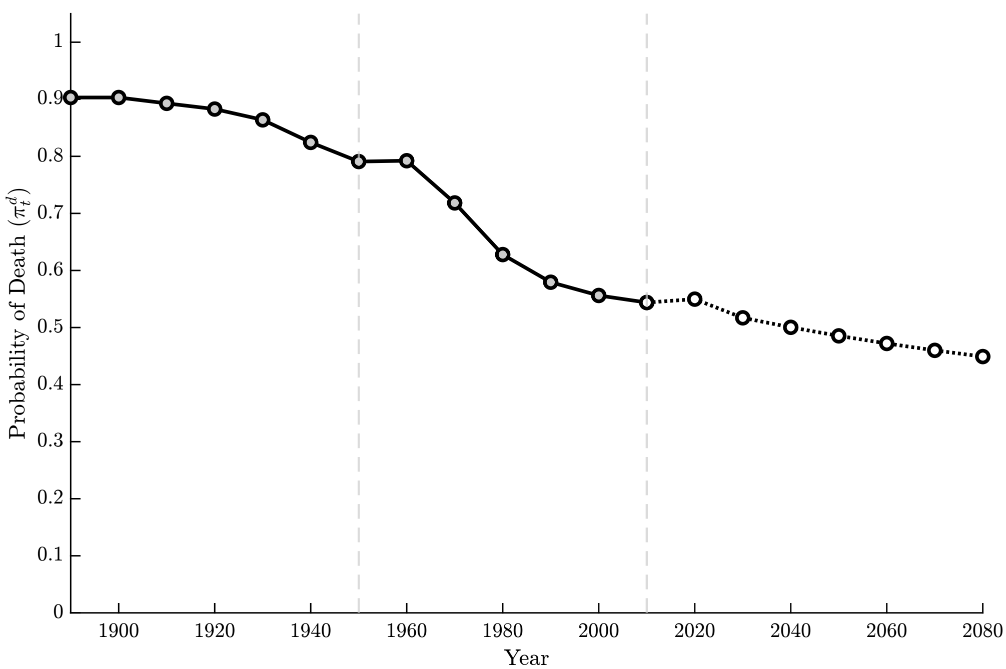


*Note:* This figure displays the decade-probability of death conditional on being retired, $\pi_t^d$, over the calendar transition path. The solid black line with circular markers represents historical values calculated by interpolating Social Security Administration (SSA) male period life tables at the average male effective retirement age provided by the Center for Retirement Research (CRR). The dotted gray line denotes the projected series. Vertical dashed lines delineate the boundaries of the 1950–2010 calibration window.

Figure C.21: Conditional Retirement Probabilities

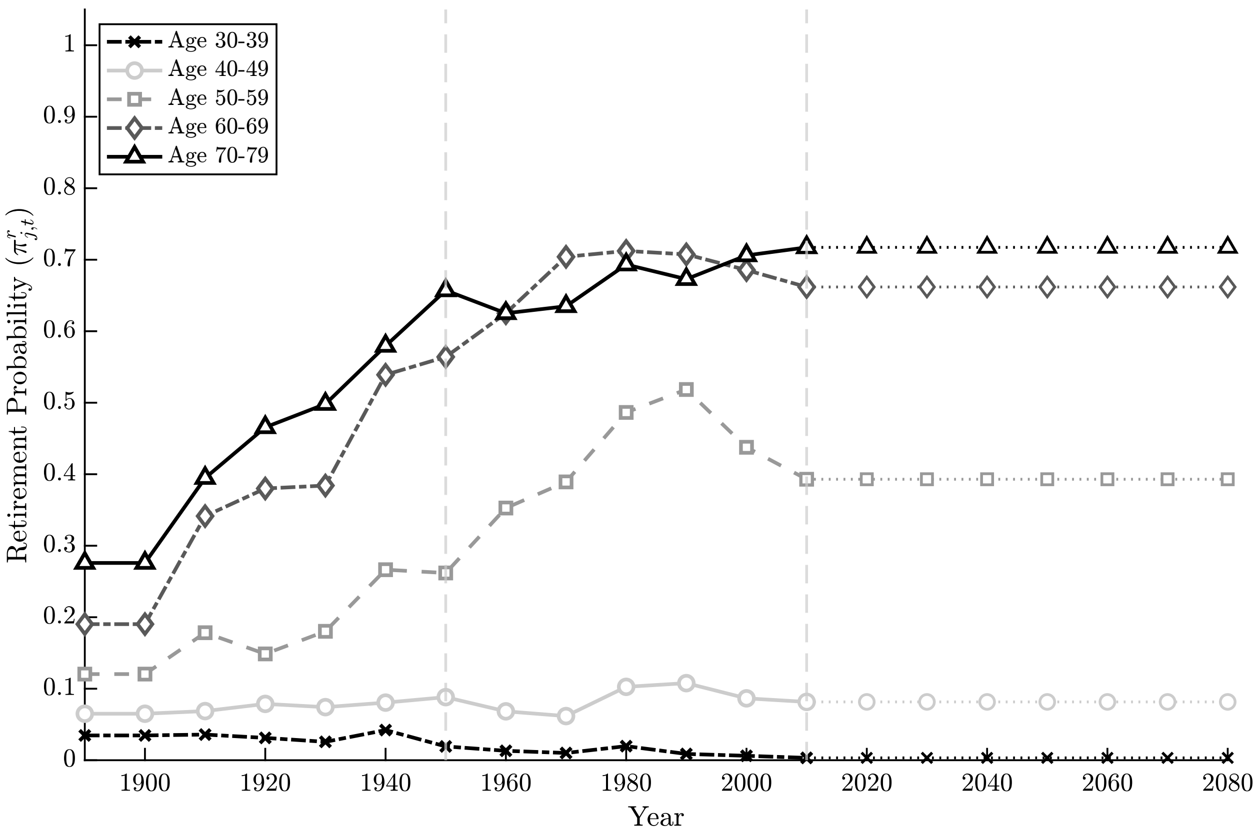


*Note:* This figure displays the conditional probability of retirement ($\pi^r_{j,t}$) over time. Probabilities are imputed using microdata from the American Community Survey (ACS). I calculate the binary labor force participation rate for the reference person (household head) in each household, aggregated by calendar decade and decadal age group. The conditional retirement risk is then backed out as the implied drop in participation between successive age decades. The plotted series focus on the 50s, 60s, and 70s age groups, where the margin of labor force exit is most active. By terminal age 80, the model imposes a retirement probability of exactly 1.0. As with other exogenous inputs, incomplete ACS data post-2020 is padded using the 2010s values (dotted lines).

Figure C.22: Wealth Endowment at 20-29 years-old

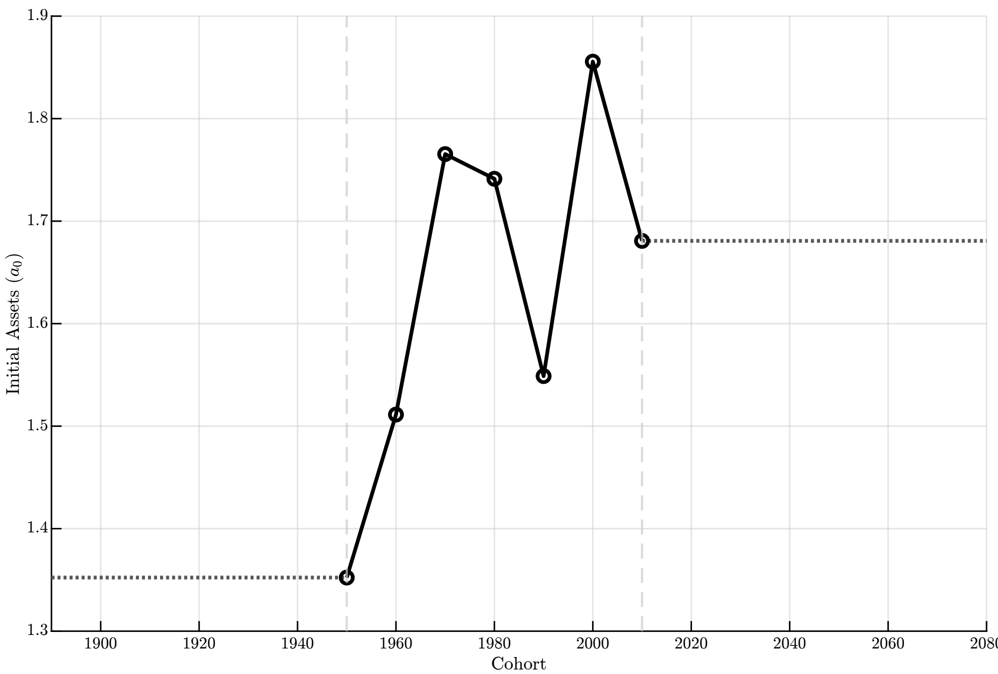


*Note:* This figure illustrates the transition path for the initial asset endowment, $a_0$, assigned to each cohort upon entry into the model at age 20. The solid black line with markers identifies the primary calibration window (1950–-2010), where $a_0$ is pinned to normalized data from the Survey of Consumer Finances. To ensure the overlapping generations (OLG) model reaches a stationary steady state both before and after the historical window, we utilize a steady-state padding scheme.

Figure C.23: Estimated Path: Discount Parameter

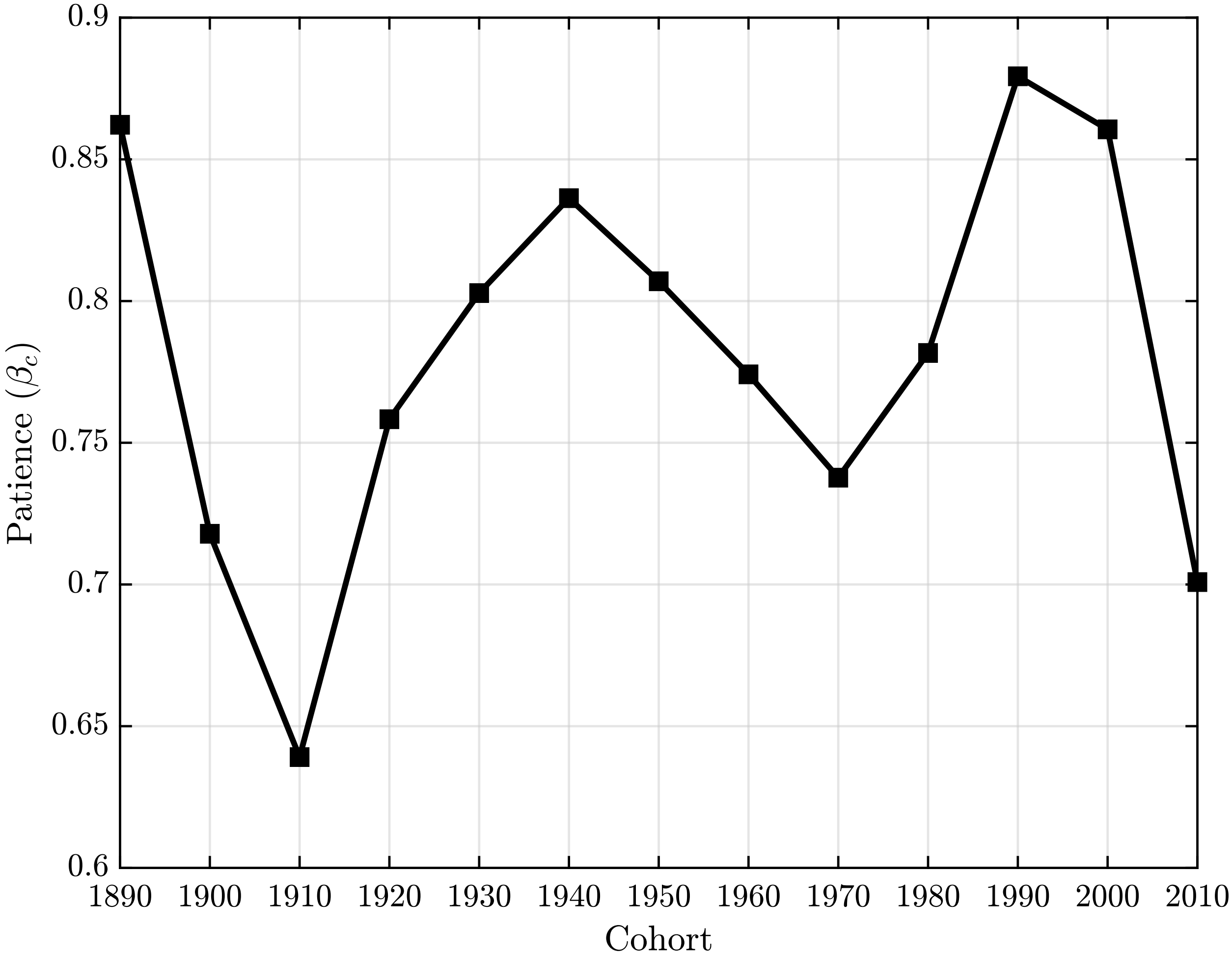


*Note:* This figure plots the estimated sequence for the discount parameter ($\beta$).

# D Appendix Tables

Table D.1: Summary Statistics

| | N | Mean (2022 USD) | Std. dev. | 50%-tile | 90%-tile |
|---|---|---|---|---|---|
| Total Assets | 112,507 | 6,891,684.65 | 51,995,284 | 168,725 | 4,309,333 |
| Financial assets (with DB) | 112,507 | 2,617,619.18 | 24,243,657 | 55,325 | 1,876,344 |
| Bonds | 112,507 | 260,225.57 | 4,388,119 | 0 | 11,167 |
| Stocks | 112,507 | 862,649.82 | 14,395,433 | 0 | 141,188 |
| Defined benefit pension | 112,507 | 108,625.45 | 552,149 | 7,460 | 162,149 |
| Certificates of deposit | 102,135 | 27,069.86 | 636,839 | 0 | 0 |
| Savings bonds | 112,507 | 5,764.60 | 218,193 | 0 | 4,291 |
| Transaction accounts | 112,507 | 220,824.80 | 3,013,161 | 6,741 | 141,851 |
| Retirement accounts | 112,507 | 187,305.68 | 1,318,662 | 0 | 305,000 |
| Life insurance | 112,507 | 40,975.06 | 646,797 | 0 | 13,268 |
| Other financial assets | 112,507 | 55,907.14 | 1,725,239 | 0 | 0 |
| Non-financial assets | 112,507 | 4,358,313.18 | 38,317,855 | 129,895 | 2,147,411 |
| Vehicles | 112,507 | 60,671.73 | 1,055,342 | 10,687 | 60,400 |
| Primary residence | 112,507 | 433,808.14 | 1,908,475 | 97,538 | 792,496 |
| Other real-estate | 112,507 | 573,617.49 | 9,057,911 | 0 | 269,837 |
| Business equity | 112,507 | 3,201,367.98 | 33,735,451 | 0 | 565,335 |
| Other nonfinancial | 112,507 | 90,243.85 | 2,825,496 | 0 | 0 |
| Total Debt | 112,502 | 164,202.03 | 2,314,822 | 9,887 | 256,815 |
| Personal debt | 112,507 | 67,331.25 | 2,119,203 | 1,110 | 36,000 |
| Credit card debt | 112,507 | 1,668.40 | 7,745 | 0 | 3,246 |
| Housing debt | 112,502 | 87,065.80 | 412,753 | 0 | 201,144 |
| Other real estate debt | 112,507 | 33,922.88 | 613,792 | 0 | 0 |
| Real other debt | 112,507 | 19,104.03 | 678,541 | 0 | 0 |
| Net Wealth | 112,507 | 6,815,193.36 | 51,422,450 | 156,335 | 4,329,856 |
| Total Income | 112,507 | 490,658.64 | 5,391,896 | 60,771 | 356,153 |
| Capital income | 102,135 | 210,363.52 | 2,836,235 | 0 | 37,729 |
| Wages sal and self Employ | 102,135 | 179,652.89 | 1,707,360 | 45,784 | 193,326 |
| Wages and salaries | 102,135 | 115,886.53 | 1,010,945 | 39,812 | 159,480 |
| Welfare and transfers | 102,135 | 15,507.13 | 868,211 | 0 | 26,135 |

*Note:* This table contains summary statistics for SCF+ data for all survey waves between 1950 and 2022. Each observation is survey wave-by-individual SCF id pair weighted by 5 imputations using SCF provided imputation weights.

Table D.2: Concentration Coefficient by Asset Class

| | (1) 1950s | (2) 1980s | (3) 2010s | (4) $\%\Delta_{1980s-1950s}$ | (5) $\%\Delta_{2010s-1980s}$ |
|---|---|---|---|---|---|
| Net Worth | 0.184 | 0.303 | 0.320 | 0.653 | 0.056 |
| Total Assets | 0.155 | 0.260 | 0.275 | 0.680 | 0.059 |
| Financial assets (with DB) | 0.253 | 0.353 | 0.338 | 0.393 | -0.043 |
| Stocks | 0.248 | 0.475 | 0.403 | 0.918 | -0.153 |
| Defined benefit pension | 0.185 | 0.342 | 0.319 | 0.845 | -0.067 |
| Bonds | 0.359 | 0.492 | 0.439 | 0.369 | -0.108 |
| Savings bonds | 0.308 | 0.387 | 0.326 | 0.254 | -0.157 |
| Cert of deposit | | 0.529 | 0.470 | | -0.112 |
| Transaction acc. | 0.278 | 0.347 | 0.259 | 0.248 | -0.252 |
| Retirement acc. | | 0.219 | 0.292 | | 0.333 |
| Life insurance | | 0.108 | 0.330 | | 2.063 |
| Money mkt acc. | | 0.349 | 0.342 | | -0.019 |
| Mutual funds | | 0.493 | 0.383 | | -0.224 |
| Other fin assets | | 0.184 | 0.326 | | 0.766 |
| Non-Financial assets | 0.101 | 0.197 | 0.215 | 0.952 | 0.095 |
| Vehicles | -0.087 | 0.020 | 0.044 | 1.224 | 1.263 |
| Primary residence | 0.120 | 0.152 | 0.172 | 0.267 | 0.133 |
| Other real-estate | 0.210 | 0.325 | 0.351 | 0.549 | 0.079 |
| Business equity | 0.091 | 0.229 | 0.231 | 1.517 | 0.009 |
| Other nonfin | | 0.061 | 0.375 | | 5.189 |
| Total Debt | -0.209 | -0.143 | -0.076 | 0.318 | 0.465 |
| Personal debt | -0.192 | -0.079 | -0.162 | 0.590 | -1.061 |
| Credit card debt | | -0.140 | 0.013 | | 1.094 |
| Housing debt | -0.214 | -0.165 | -0.060 | 0.228 | 0.636 |
| Other real estate debt | 0.043 | 0.058 | 0.086 | 0.365 | 0.465 |
| Real other debt | -0.184 | 0.155 | 0.172 | 1.842 | 0.110 |

*Note:* This table shows the concentration coefficients for each asset class. 1950s comprises the 1950, 1953, 1956, and 1959 SCF+ survey waves, the 1980s comprise the 1983 and 1989 waves, and the 2010s curve is constructed using the 2010, 2013, 2016, 2019, and 2022 waves. Non-financial assets are categorized by the SCF as physical or tangible assets that are not primarily financial in nature.

Table D.3: Coefficient Contribution by Asset Class

| | Leave-one-out | | | % of Δ from change in | | |
|---|---|---|---|---|---|---|
| | (1) 1950s | (2) 2010s | (3) Δ | (4) own coef. | (5) share of NW | (6) total |
| Net Worth | 0.184 | 0.320 | 0.137 | 100.0 | 0.0 | 100.0 |
| Total Assets | -0.209 | -0.066 | 0.143 | 97.4 | 8.3 | 105.7 |
| Financial assets (with DB) | 0.141 | 0.298 | 0.158 | 29.2 | 39.3 | 68.5 |
| Stocks | 0.165 | 0.315 | 0.150 | 15.7 | -39.0 | -23.3 |
| Defined benefit pension | 0.183 | 0.321 | 0.137 | 11.3 | 21.2 | 32.5 |
| Bonds | 0.178 | 0.319 | 0.141 | 1.3 | -5.9 | -4.6 |
| Savings bonds | 0.180 | 0.320 | 0.140 | 0.2 | -5.8 | -5.6 |
| Transaction acc. | 0.175 | 0.324 | 0.149 | -1.0 | -5.9 | -6.8 |
| Non-Financial assets | 0.374 | 0.454 | 0.080 | 52.6 | -15.9 | 36.7 |
| Vehicles | 0.192 | 0.328 | 0.137 | 2.8 | 0.0 | 2.8 |
| Primary residence | 0.210 | 0.372 | 0.162 | 10.6 | -4.1 | 6.5 |
| Other real-estate | 0.183 | 0.317 | 0.135 | 6.0 | 12.1 | 18.1 |
| Business equity | 0.232 | 0.340 | 0.108 | 26.9 | -19.3 | 7.6 |
| Total Debt | 0.155 | 0.276 | 0.121 | -10.0 | 4.9 | -5.1 |
| Personal debt | 0.177 | 0.309 | 0.132 | -0.5 | 0.9 | 0.4 |
| Housing debt | 0.161 | 0.287 | 0.127 | -8.8 | 3.4 | -5.4 |
| Other real estate debt | 0.183 | 0.318 | 0.135 | -0.3 | -0.3 | -0.6 |
| Real other debt | 0.183 | 0.320 | 0.137 | -0.4 | 0.0 | -0.4 |

*Note:* This table shows how each balance-sheet item contributes to the 1950s-to-2010s rise in the age-concentration coefficient of net worth, which rose from 0.184 to 0.320. Column (1): age-concentration coefficient of net worth with this item removed (added back, for debts), 1950s. Column (2): same, 2010s. Column (3): the change, (2)−(1). For columns (4)–(6), the coefficient of net worth is a weighted sum of the coefficients of the balance-sheet items, $C = \sum_k w_k C_k$, with $w_k$ the item's share of net worth (negative for debt) and $C_k$ its own age-concentration coefficient (as in Table D.2). Each item's contribution to the 0.137 rise splits into column (4), the change in the item's own coefficient weighted by its average share ($\bar{w}_k \Delta C_k$), and column (5), the change in the item's share of net worth weighted by its average coefficient ($\Delta w_k \bar{C}_k$); column (6) is the sum, the item's total contribution, as a percent of 0.137. Column (6) sums to 100 across any set of items that partitions net worth. Items not collected in the 1950s SCF+ waves are omitted.

## Table D.4: Population, Net Worth, and Concentration by Education

| | Share of households | | Share of net worth | | Share of $C$ | |
|---|---|---|---|---|---|---|
| | 1950s (1) | 2010s (2) | 1950s (3) | 2010s (4) | 1950s (5) | 2010s (6) |
| College | 0.158 | 0.600 | 0.325 | 0.850 | 0.264 | 0.841 |
| Non-college | 0.842 | 0.400 | 0.675 | 0.150 | 0.736 | 0.159 |

*Note:* This table reports the share of households, of aggregate net worth, and of the age-wealth concentration coefficient held by college and non-college households, where college denotes a head with at least some college. The share of $C$ splits the coefficient of equation (2) into the parts contributed by each group's wealth, with all households ranked together by age; it exceeds the group's share of net worth when that wealth is held at older positions in the ranking.

## Table D.5: Concentration Contributions by Education

| | Contribution to the rise in $C$ (% of the rise) | | | | |
|---|---|---|---|---|---|
| | Within group (1) | Between groups (2) | Joint (3) | Age position (4) | Total (5) |
| College | 14.1 | 117.3 | 22.9 | 7.3 | 161.6 |
| Non-college | 49.2 | −65.8 | −38.3 | −6.7 | −61.6 |
| Both groups | 63.3 | 51.5 | −15.4 | 0.6 | 100.0 |

*Note:* This table decomposes the rise in the age-wealth concentration coefficient from 0.184 to 0.320 into the contributions of college and non-college households, in percent of the 0.137 increase. Column (1) varies each group's own concentration coefficient holding its share of net worth at the 1950s value, column (2) does the reverse, and column (3) is the part generated by both changing at once. Column (4) is the change in the group's position in the economy-wide age ranking, which its own coefficient does not capture.

Table D.6: PARAMETERS CONSTANT ACROSS TIME

| Parameter | Description | Value | Source/Target |
|---|---|---|---|
| $\gamma$ | Coefficient of relative risk aversion | 1.125 | Chetty (2006) |
| $\sigma$ | Elasticity of substitution K and L | 0.6 | Knoblach and Stöckl (2020) |
| $\delta$ | Human Capital depreciation | 0.355 | Dinerstein et al. (2022) |
| $\alpha$ | Ret. to scale in human capital tech. | 0.212 | SMM |

Table D.7: PARAMETERS VARYING ACROSS TIME

| Parameter | Description | 1950s | 1960s | 1970s | 1980s | 1990s | 2000s | 2010s | Source/Target |
|---|---|---|---|---|---|---|---|---|---|
| $\beta$ | Cohort Patience | 0.807 | 0.774 | 0.738 | 0.782 | 0.879 | 0.861 | 0.701 | SMM |
| $\phi$ | Bequest Warm Glow | 0.243 | 0.207 | 0.327 | 0.348 | 0.386 | 0.356 | 0.331 | SMM |
| $\pi^d$ | Conditional Death Prob. | 0.791 | 0.792 | 0.718 | 0.628 | 0.579 | 0.556 | 0.544 | SSA & Munnell (2025) |
| $z$ | Human Capital Productivity | 0.613 | 0.673 | 1.050 | 1.632 | 1.713 | 1.708 | 0.841 | SMM |
| $W$ | Aggregate Wage Rate | 5.991 | 8.041 | 9.986 | 9.079 | 7.937 | 6.912 | 6.090 | SMM |
| $R$ | Return on Capital | 1.809 | 1.548 | 1.507 | 1.967 | 2.364 | 1.378 | 1.888 | Jordà et al. (2017) |
| $\pi^r_{20-29}$ | Retirement Prob. | 0.000 | 0.000 | 0.000 | 0.000 | 0.000 | 0.000 | 0.000 | CPS |
| $\pi^r_{30-39}$ | Retirement Prob. | 0.019 | 0.013 | 0.010 | 0.020 | 0.009 | 0.006 | 0.003 | CPS |
| $\pi^r_{40-49}$ | Retirement Prob. | 0.088 | 0.068 | 0.062 | 0.103 | 0.108 | 0.087 | 0.082 | CPS |
| $\pi^r_{50-59}$ | Retirement Prob. | 0.262 | 0.353 | 0.389 | 0.486 | 0.518 | 0.438 | 0.393 | CPS |
| $\pi^r_{60-69}$ | Retirement Prob. | 0.564 | 0.625 | 0.704 | 0.712 | 0.707 | 0.686 | 0.662 | CPS |
| $\pi^r_{70-79}$ | Retirement Prob. | 0.657 | 0.625 | 0.635 | 0.693 | 0.673 | 0.706 | 0.717 | CPS |
| $\pi^r_{80+}$ | Retirement Prob. | 1.000 | 1.000 | 1.000 | 1.000 | 1.000 | 1.000 | 1.000 | CPS |

Table D.8: Life-Cycle Earnings Profiles: Data vs. Model

| Age Group | 1930s | 1940s | 1950s | 1960s | 1970s | 1980s | 1990s |
|---|---|---|---|---|---|---|---|
| **Panel A: SCF Data** | | | | | | | |
| 20-29 | 4.99 | 6.68 | 7.58 | 7.85 | 7.35 | 8.29 | 8.46 |
| 30-39 | 5.65 | 7.80 | 10.17 | 10.44 | 9.88 | 11.39 | 12.64 |
| 40-49 | 5.62 | 8.42 | 10.33 | 10.60 | 12.08 | 14.33 | 14.64 |
| 50-59 | 4.90 | 6.56 | 8.36 | 9.15 | 10.26 | 14.65 | 14.22 |
| 60-69 | 2.56 | 4.39 | 5.96 | 6.91 | 6.11 | 9.35 | 11.55 |
| 70-79 | 3.53 | 2.56 | 4.48 | 4.18 | 4.76 | 6.48 | 7.74 |
| 80+ | 8.56 | 2.35 | 2.91 | 5.26 | 4.16 | 4.41 | 5.97 |
| **Panel B: Model-Implied** | | | | | | | |
| 20-29 | 5.26 | 7.24 | 9.18 | 7.92 | 6.00 | 5.72 | 5.59 |
| 30-39 | 5.57 | 7.60 | 9.82 | 10.44 | 11.75 | 12.14 | 10.64 |
| 40-49 | 5.54 | 7.70 | 9.99 | 10.83 | 13.06 | 15.20 | 14.12 |
| 50-59 | 5.25 | 6.93 | 9.42 | 10.39 | 12.14 | 13.86 | 14.18 |
| 60-69 | 3.64 | 5.12 | 5.57 | 5.98 | 6.05 | 6.23 | 7.31 |
| 70-79 | 1.79 | 1.98 | 2.25 | 1.60 | 1.85 | 1.83 | 1.79 |
| 80+ | 1.05 | 0.77 | 0.90 | 0.85 | 0.57 | 0.67 | 0.50 |

*Notes:* This table evaluates the model's fit against the historical evolution of life-cycle earnings profiles across seven decades (1950–2010). Panel A reports the empirical moments calculated from the harmonized Survey of Consumer Finances (SCF+) data. Panel B reports the corresponding moments implied by the general equilibrium path of the structural overlapping generations (OLG) model. All values are expressed in hundreds of thousands ($100,000$) of constant 2022 US dollars. Cell values denote the average real labor income earned within each specific age cohort, averaged over all survey waves within the respective decade.

Table D.9: Life-Cycle Wealth Profiles: Data vs. Model

| Age Group | 1930s | 1940s | 1950s | 1960s | 1970s | 1980s | 1990s |
|---|---|---|---|---|---|---|---|
| **Panel A: SCF Data** | | | | | | | |
| 20-29 | 1.35 | 1.51 | 1.77 | 1.74 | 1.55 | 1.86 | 1.68 |
| 30-39 | 2.12 | 3.02 | 3.67 | 4.26 | 3.83 | 5.07 | 5.40 |
| 40-49 | 2.95 | 4.62 | 4.85 | 7.13 | 8.53 | 10.38 | 10.80 |
| 50-59 | 3.28 | 4.02 | 5.27 | 8.66 | 10.70 | 16.57 | 16.03 |
| 60-69 | 2.05 | 4.91 | 3.85 | 7.02 | 8.26 | 13.74 | 15.91 |
| 70-79 | 3.39 | 2.38 | 2.96 | 4.49 | 5.32 | 9.66 | 11.98 |
| 80+ | 11.03 | 3.98 | 2.75 | 8.28 | 5.02 | 7.27 | 9.77 |
| **Panel B: Model-Implied** | | | | | | | |
| 20-29 | 1.35 | 1.51 | 1.77 | 1.74 | 1.55 | 1.86 | 1.68 |
| 30-39 | 1.59 | 2.20 | 2.87 | 4.41 | 4.30 | 3.50 | 3.78 |
| 40-49 | 2.13 | 3.05 | 4.27 | 6.41 | 8.65 | 9.67 | 9.63 |
| 50-59 | 3.11 | 3.73 | 5.40 | 8.14 | 11.53 | 15.60 | 14.91 |
| 60-69 | 2.47 | 4.18 | 4.99 | 7.35 | 10.76 | 14.95 | 16.34 |
| 70-79 | 4.03 | 2.37 | 3.97 | 4.92 | 7.38 | 11.08 | 12.91 |
| 80+ | 9.45 | 2.83 | 1.76 | 3.20 | 4.13 | 6.05 | 8.39 |

*Notes:* This table evaluates the model's fit against the historical evolution of life-cycle wealth profiles across birth cohorts from seven decades (1930s–1990s). Panel A reports the empirical moments calculated from the harmonized Survey of Consumer Finances (SCF+) data. Panel B reports the corresponding moments implied by the general equilibrium path of the structural overlapping generations (OLG) model. All values are expressed in hundreds of thousands $(100,000)$ of constant 2022 US dollars. Cell values denote the average real net worth held by households within each specific age cohort, averaged over all survey waves within the respective decade.